CHALMERS
UNIVERSITY OF TECHNOLOGY

# Spherically Symmetric Self-Gravitating Elastic Bodies

A Numerical Investigation

ASTRID LILJENBERG

Department of Mathematical Sciences
Chalmers University of Technology
Gothenburg, Sweden 2020

Thesis for the Degree of Master of Science

# Spherically Symmetric Self-Gravitating Elastic Bodies: A Numerical Investigation

Astrid Liljenberg


CHALMERS
UNIVERSITY OF TECHNOLOGY

Department of Mathematical Sciences
Chalmers University of Technology
Gothenburg, Sweden 2020

**Spherically Symmetric Self-Gravitating Elastic Bodies:**
**A Numerical Investigation**
Astrid Liljenberg



Supervisor: Simone Calogero, Department of Mathematical Sciences
Examiner: Håkan Andréasson, Department of Mathematical Sciences

Department of Mathematical Sciences
Chalmers University of Technology
SE-412 96 Gothenburg
Telephone +46 31 772 1000

Typeset in LaTeX
Printed by Chalmers Reproservice
Gothenburg, Sweden 2020

# Spherically Symmetric Self-Gravitating Elastic Bodies: A Numerical Investigation

Astrid Liljenberg

Department of Mathematical Sciences
Chalmers University of Technology

## Abstract

We investigate numerically the existence and properties of static self-gravitating elastic balls in the Euler formulation of continuum mechanics. In this formulation sufficient conditions for the existence of finite radius balls were recently derived for the Saint Venant-Kirchhoff, quasi-linear John, and Hadamard material models. Some problems were left open regarding whether or not the sufficient conditions for existence are also necessary. We find numerical evidence suggesting that the hyperbolicity condition at the center is indeed necessary, but that several other conditions on the central densities are stronger than necessary and can be replaced by weaker ones. We also find evidence of finite radius balls existing in the quasi-linear Signorini model. Furthermore, the properties of static balls in the recently introduced polytropic elastic material model are investigated and we find numerical evidence of the existence of static spherically symmetric balls, shells and multi-bodies. Mass-radius diagrams are constructed, some of which admit spiral type curves. Finally, we investigate numerically the existence and properties of time-dependent homologous solutions to the Cauchy-Poisson system for polytropic elastic balls and find that solutions exist but do not conserve mass unless static.

# Acknowledgements

First and foremost I would like to thank my supervisor Simone Calogero for the amazing support throughout the project. I would also like to thank my mother Eva for always cheering me on, and my father Per for proofreading the thesis.

Astrid Liljenberg
Gothenburg, October 16, 2020

# Contents

# 1

# Introduction

An important problem in Astrophysics is to study the equations of motion of spherically symmetric matter distributions interacting with their own self-generated gravitational field. Such models are commonly applied to a variety of physical systems, like stars, planets and galaxies. The physical and mathematical literature abound of results on the analysis of these models when the matter distribution consists of a fluid with a barotropic equation of state, see for instance [6, 10]. Fluid models are used above all to study properties of stars in the main sequence. The purpose of this thesis is to investigate numerically the dynamics of matter distributions that consist of one or more elastic bodies, e.g., planets or neutron stars [5, 14]. This investigation will be carried out using the Euler formulation of elasticity theory in spherical symmetry introduced recently in [1, 2]. In this formulation the equations of motion for spherically symmetric elastic bodies form a first order strictly hyperbolic system similar to the Euler equations for fluid balls.

The objectives of this thesis are the following:

1. Study numerically the questions left open in [1, 2] regarding the existence of static spherically symmetric elastic balls in the Saint Venant-Kirchoff, John, Hadamard, and Signorini material models.
2. Study numerically the existence and properties of static self-gravitating elastic matter distributions in the polytropic elastic material model recently introduced in [4].
3. Study numerically the existence and properties of time-dependent homologous solutions to the Cauchy-Poisson system for spherically symmetric elastic balls in the polytropic material model.

## Outline of the thesis

Chapter 2 contains the mathematical background required in the subsequent chapters. It introduces the equations of interest for general matter distributions in static equilibrium as well as the definition of self-gravitating balls of matter. The particular case of polytropic fluid balls is already well understood and is reviewed in Chapter 3, static fluid balls in Section 3.1 and time-dependent fluid balls in Section 3.2. While not directly related to the objectives of the thesis listed above, studying fluid balls will allow for interesting comparisons with elastic balls in later chapters.

Moreover, it familiarizes the reader with numerically constructed matter balls and how results are visualized and interpreted.

The elastic counterpart of Section 3.1 is contained in Chapter 4, that is, static elastic bodies. The purpose of the chapter is to complete the first two objectives above. It introduces the different elastic material models, together with the open problems and our numerical findings. Chapter 5 is the counterpart to Section 3.2, that is, it covers time-dependent homologous elastic balls. The chapter presents our numerical findings related to the third objective above.

Chapter 6 contains a summary and discussion of our numerical findings

# Method and numerics

The equations solved in this thesis are systems of nonlinear ordinary differential equations. They were solved using the solver `ode45` in Matlab (version 9.8 for Windows), which implements a Runge-Kutta based algorithm with adaptive step size. The initial data is usually given at the origin, which is a singularity for these equations. To deal with this, a second order Taylor expansion was used to approximate the initial condition at a point $\varepsilon \ll 1$ close to the origin. Matlab used this $\varepsilon$ as a starting point for the integration and terminated once the so-called radial pressure reached zero. Sample code that shows the steps in detail for one material model is included in Appendix A.

In practice, we were able to start the integration in Matlab at a point $\varepsilon$ close enough to zero that the difference between using the initial data at 0 and its approximation at $\varepsilon$ was practically non-existent and did not affect the numerical results in any way.

The gravitational constant $G$ appears frequently throughout the thesis. Because this thesis is concerned with qualitative properties of solutions more than anything else, $G$ was set to 1 during all numerical computations.

# 2

# Background

We review relevant concepts from continuum mechanics, geometry, and elasticity theory and present the equations of interest for this thesis.

## 2.1 Continuum mechanics

In Newtonian gravity the gravitational potential generated at a point $0 \neq x \in \mathbb{R}^3$ by a point mass $M$ at the origin is given by

$$U(x) = -\frac{GM}{|x|}, \tag{2.1}$$

where $G$ is the Newton gravitational constant. The force generated by the scalar field $U$ on a point mass $m_*$ located at $x \neq 0$ is given by

$$F_{\text{grav}}(x) = -m_* \nabla U(x), \quad \text{or equivalently} \quad F_{\text{grav}}(x) = -\frac{Gm_*M}{|x|^2}\frac{x}{|x|}. \tag{2.2}$$

Suppose we now replace the field generating point mass at the origin with a **static** continuum body occupying the region $\Omega \subset \mathbb{R}^3$. Let the scalar field $\rho(x)$ be its mass density. Then the total mass of the body is $M = \int_\Omega \rho(x)\, dx$ and the gravitational potential generated by the body satisfies the **Poisson equation**

$$\Delta U = 4\pi G\rho \tag{2.3}$$

with the boundary condition

$$\lim_{|x|\to\infty} U(x) = 0. \tag{2.4}$$

The solution to the boundary value problem (2.3)-(2.4) is known and given by

$$U(x) = -G\int_{\mathbb{R}^3} \frac{\rho(y)}{|x-y|}\, dy. \tag{2.5}$$

Hence,

$$\nabla U(x) = G\int_{\mathbb{R}^3} \frac{\rho(y)}{|x-y|^2}\frac{x-y}{|x-y|} dy \tag{2.6}$$

and the force exercised by the body on a point particle with mass $m_*$ located at the point $x$ in the exterior of the body is

$$F_{\text{grav}}(x) = -m_* G \int_{\mathbb{R}^3} \frac{\rho(y)}{|x-y|^2} \frac{x-y}{|x-y|} dy. \tag{2.7}$$

Note that since $\rho$ is supported in $\Omega$, the domain of integration can be replaced by $\Omega$.

Let $x \in \Omega$ be a point in the interior of the body and consider an infinitesimal region of volume $dV$ around $x$. This region approximates a point particle of mass $m_* = \rho(x)dV$ at $x$. Then the force generated by the body on this region is $F_{\text{grav}}(x) = -\rho(x)dV\nabla U$. If no external forces are present the body is said to be **self-gravitating**.

A self-gravitating body in static equilibrium requires an additional inner force field $F_{\text{matter}}$ that balances out $F_{\text{grav}}$. In continuum mechanics this fundamental field acting on a microscopic level is approximated by a phenomenological field called the **matter stress field** which depends on the material of the body. We shall assume that the body is **homogeneous**, i.e., it is made of only one material. Let $\sigma(x)$ denote the matter stress field inside the body. It is a second order tensor field with components denoted by $\sigma_{ij}(x)$, $i, j = 1, 2, 3$.

The matter force acting on the region $dV$ around the point $x \in \Omega$ is defined as $F_{\text{matter}}(x) = \nabla \cdot \sigma(x)\, dV$, where $\nabla \cdot \sigma$ denotes the divergence of the second order tensor $\sigma$, i.e., the vector field with components

$$(\nabla \cdot \sigma(x))_i = \sum_{j=1}^{3} \partial_j \sigma_{ij}(x).$$

The condition for static equilibrium of a self-gravitating body becomes that

$$\nabla \cdot \sigma(x) = \rho(x)\nabla U(x) \quad \text{for all } x \in \Omega, \tag{2.8}$$

where $\nabla U$ is given by (2.6). This is called the **static Cauchy-Poisson system**.

## 2.2 Spherical symmetry

We define what it means for a scalar field or vector field to be **spherically symmetric**.

**Definition 1.** *A function $U : \mathbb{R}^3 \to \mathbb{R}$ is said to be spherically symmetric if $U(Ax) = U(x)$, for all rotations $A \in SO(3)$. A vector field $v : \mathbb{R}^3 \to \mathbb{R}^3$ is spherically symmetric if $A^T v(Ax) = v(x)$ for all $A \in SO(3)$.*

Since any vector $x = (x_1, x_2, x_3) \in \mathbb{R}^3$ can be transformed to a vector $Ax = (r, 0, 0)$, where $r = |x|$, the density distribution $\rho(x)$ of a spherically symmetric body depends only on the distance $r = |x|$ from the origin. This means that $\rho(x) = \widetilde{\rho}(r)$ for some function $\widetilde{\rho} : [0, \infty) \to [0, \infty)$. By abuse of notation we write $\rho(x) = \widetilde{\rho}(r) = \rho(r)$. The support of $\rho$ is either a **ball** of radius $R$ in which case $\Omega = \{x \in \mathbb{R}^3 : |x| \leq R\}$, or a **shell** with inner radius $R_1$ and outer radius $R_2$ in which case $\Omega = \{x \in \mathbb{R}^3 : R_1 \leq |x| \leq R_2\}$. Similarly, when a vector field $v(x)$ is spherically symmetric there

exists a $\widetilde{v} : (0, \infty) \to \mathbb{R}$ such that $v(x) = \widetilde{v}(r)x/r$. Again by abuse of notation we write $v(x) = v(r)x/r$.

We have a similar definition of spherically symmetric second order tensors.

**Definition 2.** *Let $\mathbb{R}^{3\times3}$ be the space of $3 \times 3$ matrices with real entries. A second order tensor field $\sigma : \mathbb{R}^3 \to \mathbb{R}^{3\times3}$ is said to be spherically symmetric if $A^T\sigma A(Ax) = \sigma(x)$ for all $A \in SO(3)$.*

It is a well known fact that a general second order tensor $\sigma$ in Cartesian coordinates is spherically symmetric if and only if

$$\sigma_{ij}(x) = \sigma_1(r)\frac{x_i x_j}{r^2} + \sigma_2(r)\left(\delta_{ij} - \frac{x_i x_j}{r^2}\right), \tag{2.9}$$

for some functions $\sigma_1, \sigma_2$, where $\delta_{ij}$ is the Kronecker delta [1]. Applying this fact to the stress tensor we can write the stress field of a generic spherically symmetric body as

$$\sigma_{ij}(x) = -p_{\text{rad}}(r)\frac{x_i x_j}{r^2} - p_{\text{tan}}(r)\left(\delta_{ij} - \frac{x_i x_j}{r^2}\right), \tag{2.10}$$

where $p_{\text{rad}}$ and $p_{\text{tan}}$ are the radial and tangential pressures of the body. By combining (2.8) and (2.10) the equation for static equilibrium of self-gravitating spherically symmetric body of matter becomes

$$\frac{dp_{\text{rad}}}{dr} = -\frac{2}{r}(p_{\text{rad}} - p_{\text{tan}}) - G\rho\frac{m}{r^2}, \quad m(r) = 4\pi\int_0^r \rho(s)s^2 ds. \tag{2.11}$$

We are interested in solutions to (2.11) that represent balls of matter so we end this section by giving a precise mathematical definition of a spherically symmetric self-gravitating ball [1].

**Definition 3.** *A triple $\mathfrak{B} = (\rho, p_{rad}, p_{tan})$ is called a strongly regular static self-gravitating ball of matter if there exists a constant $R > 0$ such that $\Omega \coloneqq \text{Int}\{r > 0 : \rho(r) > 0\} = (0, R)$ and*

*(i)* $(\rho, p_{\text{rad}}, p_{\text{tan}}) \in C^1([0, R])$ *satisfy* (2.11) *for* $r \in (0, R)$,

*(ii)* $p_{\text{rad}}(r), p_{\text{tan}}(r)$ *are positive for* $r \in [0, R)$,

*(iii)* $p_{\text{rad}}(R) = 0$,

*(iv)* $p_{\text{rad}}(0) = p_{\text{tan}}(0)$,

*(v)* $\rho(r) = p_{\text{rad}}(r) = p_{\text{tan}}(r) = 0$, *for* $r > R$,

*(vi)* $\lim_{r\to0^+} \rho'(r) = \lim_{r\to0^+} p'_{\text{rad}}(r) = \lim_{r\to0^+} p'_{\text{tan}}(r) = 0$.

Note that only the radial pressure is required to vanish on the boundary, not the tangential pressure or the mass density.

Investigating static balls made of fluid and elastic matter are the topics of Chapters 3 and 4 respectively, but first we define what we mean by elastic matter.

## 2.3 Elasticity

We begin by defining elastic matter in the **Lagrangian formulation** of continuum mechanics [1, 13].

Consider a body with open and bounded **reference configuration** $\mathcal{B} \subset \mathbb{R}^3$ and smooth boundary. A **deformation** is a orientation-preserving mapping $\phi : \overline{\mathcal{B}} \to \mathbb{R}^3$ that maps each point in the material to a point in space. The matrix of partial derivatives $F = \nabla\phi$ is called the deformation gradient and satisfies $\det F > 0$.

The tensor $C = F^T F$ is known as the right Cauchy-Green deformation tensor and has eigenvalues $\lambda_1^2, \lambda_2^2, \lambda_3^2$. The values $\lambda_1, \lambda_2, \lambda_3$ are called principal stretches and measures the amount of strain in each principal direction in a deformation.

On the reference configuration of a static self-gravitating body we define the reference mass density $\rho_{\text{ref}} : \overline{\mathcal{B}} \to (0, \infty)$ and the second order tensor field $P$ defined by

$$\nabla \cdot P(X) = G\rho_{\text{ref}}(X) \int_{\mathcal{B}} \rho_{\text{ref}}(Y) \frac{\phi(X) - \phi(Y)}{|\phi(X) - \phi(Y)|^3} dY, \quad X \in \mathcal{B}, \tag{2.12}$$

called the **first Piola-Kirchhoff stress tensor**. When it can be written as

$$P(X) = \widehat{P}(X, F(X)), \quad X \in \mathcal{B}, \tag{2.13}$$

the body is said to be made of **elastic** material with constitutive function $\widehat{P}$.

In the deformed state of the body the mass density $\rho$ and stress tensor $\sigma$ are given by

$$\rho(\phi(X)) = \frac{\rho_{\text{ref}}}{\det F(X)}, \quad \sigma(\phi(X)) = \frac{\widehat{P}(X, F(X))F^T(X)}{\det F(X)}, \tag{2.14}$$

at the point $x = \phi(X)$ [1].

A material is

- **hyperelastic** if there exists a function $W$, called the stored energy function, such that $\widehat{P}(F) = \rho_{\text{ref}}(\partial W / \partial F)$.
- **frame indifferent** if $\widehat{P}(X, AF) = A\widehat{P}(X, F)$, for all $A \in SO(3)$.
- **homogeneous** if $\widehat{P}$ does not explicitly depend on $X$, that is, $P(X) = \widehat{P}(F(X))$ and $\rho_{\text{ref}}(X) = \mathcal{K}$.
- **isotropic** if $\widehat{P}(X, F) = \widehat{P}(X, AF)$, for all $A \in SO(3)$.

A hyperelastic material is frame indifferent, homogeneous, and isotropic if and only if the stored energy function can be written as $W(F) = \Phi(\lambda_1, \lambda_2, \lambda_3)$ for some symmetric function $\Phi$, where $\lambda_1, \lambda_2, \lambda_3$ are the principal stretches [13].

It is important that nonlinear elastic material models are consistent with linear elasticity theory for small deformations. For this reason the stored energy function of a hyperelastic material must satisfy

$$\frac{\partial^2 \Phi}{\partial \lambda_i \partial \lambda_j}(1, 1, 1) = \lambda + 2\mu\delta_{ij}, \tag{2.15}$$

for some $\lambda$ and $\mu$, called Lamé material constants [15]. More about these later.

In engineering applications the reference configuration of an elastic body could for example be a beam at rest. When a weight is placed on the beam it deforms. In astrophysics elastic bodies of interest are typically planets. They differ from beams in the sense that the original reference configuration of a planet is not observable. Planets have already been deformed by their own gravitational forces and it is not only impossible to temporarily "switch off" gravity, such a reference state has never actually existed. This is one of several reasons why it is impractical to work in terms of reference configurations for self-gravitating elastic bodies.

In [1] a more detailed discussion is given on the drawbacks of the Lagrangian formulation, and it goes on to introduce an alternative definition of static self-gravitating elastic bodies in the **Euler formulation** of continuum mechanics. An important limitation of this definition is that it is only equivalent to the Lagrangian one for spherically symmetric bodies. It defines a (spherically symmetric) static self-gravitating elastic body as follows [1, 2]:

**Definition 4.** *Let $\mathfrak{B} = (\rho, p_{\text{rad}}, p_{\text{tan}})$ be a strongly regular static, self-gravitating ball supported in $[0, R]$; let*

$$m(r) = 4\pi \int_0^r s^2 \rho(s)\, ds, \quad r \in [0, R]$$

*be the local mass of the ball. Given a constant $\mathcal{K} > 0$ and two functions $\widehat{p}_{\text{rad}}, \widehat{p}_{\text{tan}} : (0, \infty)^2 \to \mathbb{R}$ independent of $\mathcal{K}$, we say that $\mathfrak{B}$ is made of* **homogeneous elastic matter***, or simply to be an* **elastic ball***, with* **constitutive functions** *$\widehat{p}_{\text{rad}}, \widehat{p}_{\text{tan}}$ and that $\mathfrak{B}$ has* **reference density** *$\mathcal{K} > 0$ if the radial and tangential pressures have the form*

$$p_{\text{rad}}(r) = \widehat{p}_{\text{rad}}(\delta(r), \eta(r)), \quad p_{\text{tan}}(r) = \widehat{p}_{\text{tan}}(\delta(r), \eta(r)),$$

*where*

$$\delta(r) = \frac{\rho(r)}{\mathcal{K}}, \quad \eta(r) = \frac{m(r)}{\frac{4\pi}{3}\mathcal{K} r^3}, \quad r \in (0, R).$$

*If there exists a function $w : (0, \infty)^2 \to \mathbb{R}$ such that $w(1, 1) = 0$ and*

$$\widehat{p}_{\text{rad}}(\delta, \eta) = \delta^2 \partial_\delta w(\delta, \eta), \quad \widehat{p}_{\text{tan}}(\delta, \eta) = \widehat{p}_{\text{rad}}(\delta, \eta) + \frac{3}{2}\delta\eta\partial_\eta w(\delta, \eta), \tag{2.16}$$

*then the body is said to be made of* **hyperelastic** *matter, or to be an* **hyperelastic ball***, with* **stored energy function** *$w$.*

*Remark.* Note that $\lim_{r\to 0^+} \delta(r) = \lim_{r\to 0^+} \eta(r) =: \delta_c$ and that condition (iv) in Definition 3 is satisfied for all values of the central density $\rho_0 = \rho(0)$ if and only if

$$\widehat{p}_{\text{rad}}(\delta, \delta) = \widehat{p}_{\text{tan}}(\delta, \delta). \tag{2.17}$$

The reference density $\mathcal{K}$ is the only connection left to the reference configuration. In the reference state $\rho = \mathcal{K}$ and thus $\delta = \eta = 1$. We impose that the reference state should be a stress-free state, i.e., that the constitutive functions must satisfy

the **natural state reference condition**

$$\widehat{p}_{\text{rad}}(1,1) = \widehat{p}_{\text{tan}}(1,1) = 0. \tag{2.18}$$

Furthermore, in order for the models to be consistent with linear elasticity for small deformations, we also have the following conditions on the constitutive functions [1]:

$$\partial_\delta \widehat{p}_{\text{rad}}(1,1) = \lambda + 2\mu, \quad \partial_\eta \widehat{p}_{\text{rad}}(1,1) = -\frac{4}{3}\mu, \tag{2.19a}$$

$$\partial_\delta \widehat{p}_{\text{tan}}(1,1) = \lambda, \quad \partial_\eta \widehat{p}_{\text{tan}}(1,1) = \frac{2}{3}\mu, \tag{2.19b}$$

which are equivalent to (2.15).

## 2.4 Equations of motion

Previously we have only considered static bodies, but there is a more general system of equations for the motion of self-gravitation balls called the Cauchy-Poisson system. It is given by

$$\partial_t \rho + \frac{1}{r^2}\partial_r(r^2 \rho u) = 0, \tag{2.20a}$$

$$\rho(\partial_t u + u\partial_r u) = -\partial_r p_{\text{rad}} + \frac{2}{r}(p_{\text{tan}} - p_{\text{rad}}) - G\rho\frac{m}{r^2}, \tag{2.20b}$$

where

$$m(t,r) = 4\pi \int_0^r \rho(t,s)\, s^2\, ds, \tag{2.20c}$$

and where $\rho, p_{\text{rad}}, p_{\text{tan}}$ are respectively the mass density, radial pressure and tangential pressure of the body. The new quantity $u \in \mathbb{R}$ is the **velocity field** of the body, which gives the velocity of each point in its interior. Since a spherically symmetric body can only expand or collapse, $u$ is a **radial velocity**. Equation (2.20a) is called the **continuity equation**. It implies that the total mass of the system, $M = m(t,\infty)$, is conserved. Note that all functions now depend not only on $r > 0$ but also on $t > 0$. When they don't, and when $u = 0$, we go back to the system (2.11) for static self-gravitating bodies.

We are interested in solutions to (2.20) that represent balls of matter so we give the following definition which is a generalization of Definition 3 of a static ball.

**Definition 5.** *Let $T > 0$. A quadruple $\mathfrak{B} = (\rho, p_{\text{rad}}, p_{\text{tan}}, u) : [0,T] \times [0,\infty) \to \mathbb{R}^4$ is said to be a strongly regular ball of matter if there exists $R : [0,T] \to (0,\infty)$ such that $R \in C^1([0,T])$ and, for all $t \in [0,T]$,*

*(i)* $\Omega(t) := \text{Int}\{r > 0 : \rho(t,r) > 0\} = (0, R(t))$;

*(ii)* $(\rho, p_{\text{rad}}, p_{\text{tan}}, u) \in C^1(\overline{\Omega_T})$, *where* $\Omega_T := \cup_{t\in[0,T]}\Omega(t)$;

*(iii)* $p_{\text{rad}}$, $p_{\text{tan}}$ *are positive in* $\Omega_T$ *and at* $r = 0$;

*(iv)* $\rho = p_{\text{rad}} = p_{\text{tan}} = u = 0$, *for* $(t,r) \in [0,T] \times [0,\infty) \setminus \overline{\Omega_T}$;

*(v)* $p_{\mathrm{rad}}(t,0) = p_{\tan}(t,0)$, $\partial_t p_{\mathrm{rad}}(t,0) = \partial_t p_{\tan}(t,0)$ *and* $u(t,0) = \partial_t u(t,0) = 0$*;*

*(vi)* $\lim_{r\to 0^+} \partial_r \rho(t,r) = \lim_{r\to 0^+} \partial_r p_{\mathrm{rad}}(t,r) = \lim_{r\to 0^+} \partial_r p_{\tan}(t,r) = 0$, *and*

$$\lim_{r\to 0^+} \partial_r u(t,r) = \lim_{r\to 0^+} u(t,r)/r := \omega_c(t), \quad \omega_c \in C([0,T]). \tag{2.21}$$

*If in addition* $\rho, p_{\mathrm{rad}}, p_{\tan}, u$ *solve* (2.20) *for* $(t,r) \in \Omega_T$ *and*

$$p_{\mathrm{rad}}(t,R(t)) = 0, \tag{2.22}$$

$$u(t,R(t)) = \dot{R}(t) \tag{2.23}$$

*then we call* $\mathfrak{B}$ *a self-gravitating strongly regular ball.*

*Remark.* Conditions (v) and (vi) are required for the stress tensor (2.10) to be differentiable at $r = 0$. The first boundary condition (2.22) means that the ball is surrounded by vacuum. The second boundary condition (2.23) means that the boundary of the ball is comoving with the matter and is required for the total mass of the ball to be conserved.

Solutions to (2.20) representing fluid and elastic balls in motion are the topics of Chapters 3 and 5 respectively.

# 3

# Self-Gravitating Fluid Balls

This chapter provides a review of self-gravitating static and time-dependent fluid balls. Studying fluid balls will allow us to compare the results for elastic balls and fluid balls. Moreover, it familiarizes the reader with numerically constructed matter balls and how their properties are visualized and interpreted.

## 3.1 Static fluid balls

A body is said to be made of **perfect fluid** matter if the matter stress field has the form $\sigma(x) = -p(x)\mathbb{I}$, where $\mathbb{I}$ is the $3 \times 3$ identity matrix and $p(x)$ is a non-negative scalar field called the **pressure** of the fluid and defined in the interior of the body. In spherical symmetry this is equivalent to letting $p_{\text{rad}} = p_{\text{tan}} = p$ in equation (2.11). Thus, the balance of force equation for a perfect fluid becomes

$$\frac{dp(r)}{dr} = -G\rho(r)\frac{m(r)}{r^2}, \quad m(r) = 4\pi \int_0^r \rho(s)s^2\, ds. \tag{3.1}$$

Definition 3 of a self-gravitating ball is reduced to the following for a perfect fluid:

**Definition 6.** *A pair $(\rho(r), p(r))$ is said to be a strongly regular static self-gravitating fluid ball if there exists $R > 0$ such that $\rho, p \in C^1([0, R])$, $\rho(r), p(r) > 0$ for $r \in [0, R)$, $\rho'(0) = p'(0) = 0$, $p(R) = 0$ and $(\rho, p)$ solve (3.1) for $r \in (0, R)$. The positive number $R$ is the radius of the ball.*

*Remark.* The pressure, $p$, vanishes on the boundary because the body is surrounded by vacuum, but the density, $\rho$, does not necessarily vanish on the boundary.

*Remark.* Note that (3.1) cannot admit shell type solutions since it would require $p(R_1) = p(R_2) = 0$ and $p(r) > 0$ for $r \in (R_1, R_2)$, but the right-hand side of (3.1) is negative meaning $p$ is decreasing.

It can be proved that, under rather mild regularity assumptions, solutions of (2.8) are necessarily spherically symmetric for perfect fluids, thus considering only (3.1) is not really a restriction, see [11].

Note that (3.1) has two unknowns. We must close the system by relating $p$ and $\rho$. In the fluid case closing the equation is done by adding a so called **equation of state** which corresponds to the constitutive functions in the elastic case.

**Definition 7.** *A perfect fluid is said to be a* **barotropic fluid** *if there exists a $C^1$ function $\widehat{p} : [0, \infty) \to [0, \infty)$ such that $p(r) = \widehat{p}(\rho(r))$. If $\widehat{p}(\rho) = c\rho^{1+1/n}$ for some*

*positive constants $c, n$, then the barotropic fluid is called a* **polytropic fluid** *with polytropic index $n$.*

Equation (3.1) for barotropic fluids reduces to an integro-ordinary differential equation on the mass density $\rho$, namely

$$\frac{d\rho(r)}{dr} = -G(\widehat{p}\,'(\rho(r)))^{-1}\rho(r)\frac{m(r)}{r^2}, \quad m(r) = 4\pi\int_0^r \rho(s)s^2\,ds, \tag{3.2}$$

provided $\widehat{p}\,'(\rho) > 0$ for $\rho > 0$. The latter holds in particular for polytropic fluids.

*Remark.* Solutions to (3.2) representing polytropic fluid balls only exist locally up to the radius $R$.

So, now the problem of interest can be rigorously formulated as follows:

**Problem**: *Given an equation of state $\widehat{p}(\rho)$ such that $\widehat{p}\,'(\rho) > 0$ and a constant $\rho_c > 0$ prove that there exists a unique solution $\rho(r)$ of (3.2) with the following properties: $\rho(0) = \rho_c$ and there exists (a necessarily unique) $R > 0$ such that $\rho > 0$ for $r \in [0, R)$, $\rho(r) = 0$ for $r > R$, $\rho \in C^1([0, R])$, $\rho'(0) = 0$ and $p(R) = \widehat{p}(\rho(R)) = 0$.*

The quantity $\rho_c = \rho(0)$ is the **central density** of the ball. It is the "initial datum" that we need to prescribe to have a unique solution of (3.2). The above problem has been discussed in many papers and is by now well-understood. In the case of polytropic equations of state we have the following theorem proved by Makino [12]. The result was later generalized and the proof considerably simplified by many authors, see e.g. [16].

**Theorem 1** ([12])**.** *A unique self-gravitating fluid ball with central density $\rho(0) = \rho_c > 0$ and polytropic equation of state $\widehat{p}(\rho) = c\rho^{1+1/n}$ exists if and only if $0 < n < 5$.*

*Remark.* Polytropic fluid balls with $n \in (0, 1)$ are not strongly regular, because $\rho'(r) \to -\infty$ as $r \to R^-$, see [17].

We have solved equation (3.2) for polytropic equation of state and polytropic indices $n = 0.5, 1.5, 3.5$ and central density $\rho_c = 1$. The density profiles of the three different fluid balls are plotted against their normalized radii in Figure 3.1. For larger polytropic indices we see that the mass is more heavily concentrated in the center of the ball.

Furthermore, we have produced so called mass-radius diagrams for the polytropic indices $n = 0.5, 1, 1.5, 3$, see Figure 3.2. This is done by solving equation (3.2) for a large set of central densities, $\rho_c$, and computing the mass and radius of each solution and plot as a point in the diagram. The resulting curve then shows the possible combinations of mass and radius for balls of that particular material. We see that, generally speaking, smaller indices may be used to model relatively small but dense polytropic balls and conversely for larger indices. For fluid balls there is typically a one-to-one correspondence between the radius and mass as can be seen in Figures 3.2a and 3.2c. There are however two interesting exceptions: when $n = 1$ the radius is independent of the mass and when $n = 3$ the mass is independent of the radius, see Figures 3.2b and 3.2d.

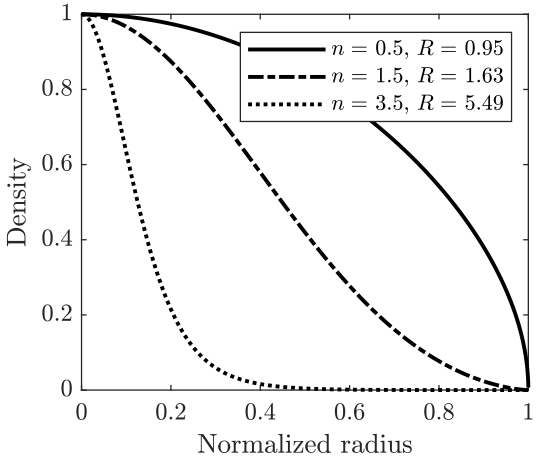


**Figure 3.1:** Density distributions for three different polytropic fluid balls with central density $\rho_c = 1$. The radii have been normalized to 1 to better illustrate the differences.

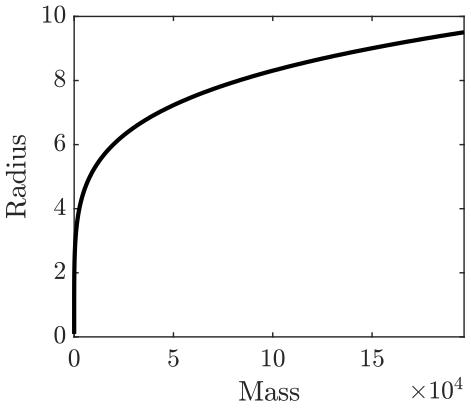


**(a)** $n = 0.5$.

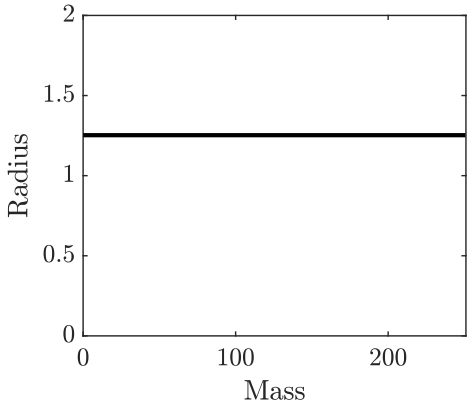


**(b)** $n = 1$.

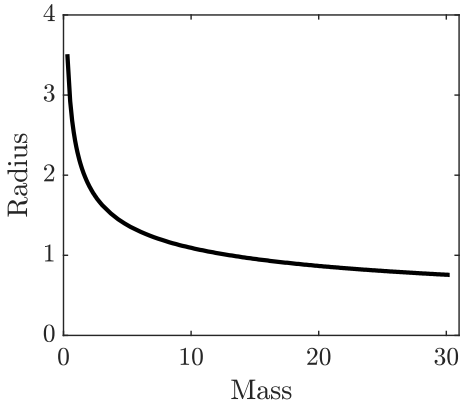


**(c)** $n = 1.5$.

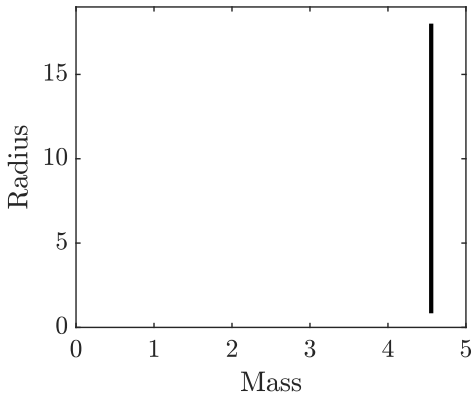


**(d)** $n = 3$.

**Figure 3.2:** Mass-radius diagrams for polytropic balls with three different polytropic indices and central densities $\rho_c \in [0.01, 100]$.

## 3.2 Time-dependent fluid balls

For polytropic fluids $p_{\text{rad}} = p_{\text{tan}} = p$ and the Cauchy-Poisson system (2.20) for balls in motion is reduced to the **Euler-Poisson** system given by

$$\partial_t \rho + \frac{1}{r^2}\partial_r(r^2 \rho u) = 0, \tag{3.3a}$$

$$\rho(\partial_t u + u\partial_r u) = -\partial_r p - G\rho\frac{m}{r^2}, \tag{3.3b}$$

where

$$p(t,r) = c\rho(t,r)^{1+\gamma}, \tag{3.3c}$$

and $\gamma = 1/n$ where $n$ is the polytropic index. Solutions of the form,

$$\rho(t,r) = \frac{1}{\phi(t)^3}\rho_0\left(\frac{r}{\phi(t)}\right), \quad u(t,r) = \frac{\dot{\phi}(t)}{\phi(t)}r, \quad \phi(t) \neq 0, \tag{3.4}$$

where $\rho_0, \phi : (0,\infty) \to (0,\infty)$, are called **homologous**, and have been studied in [9]. With this ansatz equation (2.20b) becomes

$$z\rho_0(z)\frac{\ddot{\phi}(t)}{\phi(t)} = -c(1+\gamma)\phi(t)^{-2-3\gamma}\rho_0(z)^\gamma \rho_0'(z) - \frac{G}{\phi(t)^3}\rho_0(z)\frac{m_0(z)}{z^2}, \tag{3.5}$$

where $z = r/\phi(t)$ and $m_0(z) = 4\pi\int_0^z \rho_0(s)\, s^2\, ds$. By separating the $z$ and $t$ dependence one will note that (3.5) may have solutions if and only if $\gamma = 1/3$ and $\rho_0$ and $\phi$ satisfy

$$\ddot{\phi} = \alpha G\phi^{-2}, \tag{3.6}$$

$$\rho_0' = -\theta z\rho_0^{2/3}\left(\frac{m_0}{z^3} + \alpha\right), \quad \theta = \frac{3G}{4c}, \tag{3.7}$$

for some constant $\alpha \in \mathbb{R}$. Now, (3.6) needs initial data $\phi_0 = \phi(0)$ and $\phi_1 = \dot{\phi}(0)$ and (3.7) needs a center datum $\rho_0^c > 0$. Without loss of generality we let $\phi_0 = 1$ so that $\rho_0$ is the initial datum of $\rho$.

By boundary condition (2.22), $R(t)$ is the radius at which the pressure vanishes. In polytropic fluids the pressure vanishes when $\rho(t,r) = 0$ which, by the ansatz, happens when $\rho_0(z) = 0$. If $\rho_0(z)$ has a finite radius $Z$, then $R(t)/\phi(t) = Z$ must hold at all times. Together with the ansatz for $u$, this yields that $u(t,R(t)) = \dot{R}(t)$. This means that the second boundary condition (2.23), which ensures mass conservation, is automatically satisfied for homologous polytropic fluids.

Since $R(t) = Z\phi(t)$, studying $\phi(t)$ will tell us whether a ball is expanding or collapsing over time. Solutions to (3.6) have been studied in [7] and can be summarized as follows.

**Theorem 2** ([7])**.** *Let $\phi(t)$ be the solution of (3.6) and let $\phi(0) = 1$ and $\dot{\phi}(0) = \phi_1$. Then the following holds.*

1. *If $\alpha > 0$, then $\phi(t) > 0$ for all $t > 0$ and $\phi(t) \to \infty$ as $t \to \infty$.*

2. *If $\alpha = 0$, then $\phi(t) = \phi_1 t + 1$.*

3. *If $\alpha < 0$, there exists a critical value $\phi_1^* = \sqrt{2|\alpha|G}$. If $\phi_1 \geq \phi_1^*$ then $\phi(t) > 0$ for all $t > 0$ and $\phi(t) \to \infty$ as $t \to \infty$. If $\phi_1 < \phi_1^*$, $\phi(t)$ only exists locally, that is, there exists a $T$ such that $\phi(t) > 0$ in $(0, T)$ and $\phi(t) \to 0$ as $t \to T^-$.*

In case 1 the ball could initially expand or collapse but will eventually start to expand and its radius tends to infinity. In case 2 and 3 the ball will, depending on $\phi_1$, either expand forever or collapse and form a singularity in finite time due to $\phi$ only existing locally. In the latter case, as the time approaches $T$ the radius of the ball tends to zero while the density tends to infinity. The ball could also be static in the special case $\alpha = \phi_1 = 0$.

We have solved equation (3.6) for solutions of type 1 and 3 to give examples of what $\phi$ can look like, see Figure 3.3. We have also solved instances of both equations (3.6) and (3.7) and put the solutions together to form the density $\rho(t, r)$. Figures 3.4 and 3.5 shows the time evolution of a collapsing and an expanding ball respectively. The total mass is conserved over time as expected.

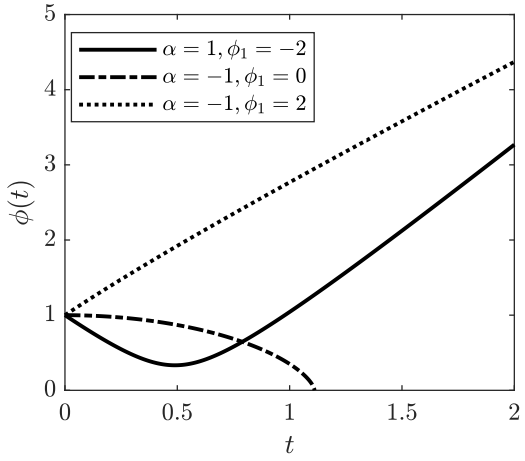


**Figure 3.3:** The behavior of $\phi(t)$ for three different combinations of $\alpha$ and $\phi_1$. The solid line corresponds to an eventually expanding solution of type 1, while both the dashed and the dotted lines correspond to solutions of type 3, one expanding and one collapsing.

Fluid balls are commonly used to model stars. The existence of collapsing fluid ball solutions whose radius tends to zero in finite time predicts the existence of singularities in black holes formed by collapsing stars. It has been conjectured that such singularities cannot form in the case of elastic bodies. Finding and studying homologous solutions to the Cauchy-Poisson system for elastic balls is the topic of Chapter 5.

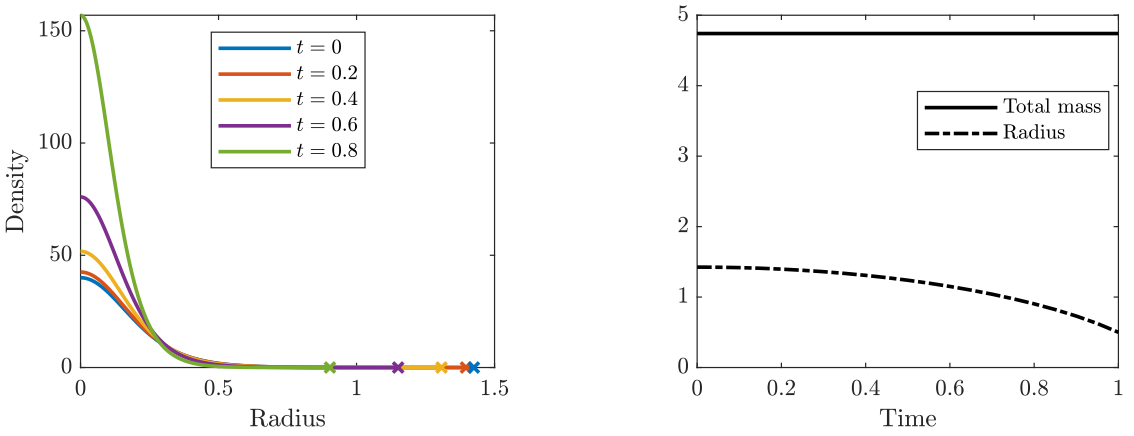


**Figure 3.4:** The pictures show the time evolution of a fluid ball with $\alpha = -1$, $\phi_1 = 0$, and $\rho_0^c = 40$. For clarity, crosses have been marked on the x-axis in the left picture to indicate where each curve ends, that is, they indicate the radius of the ball at each time step. When $\alpha = -1$, the critical value for $\phi_1$ is $\sqrt{2}$, so the ball will collapse and form a singularity in finite time. The y-axis in the right picture is not labeled because we have plotted both the total mass and the radius despite the different units.

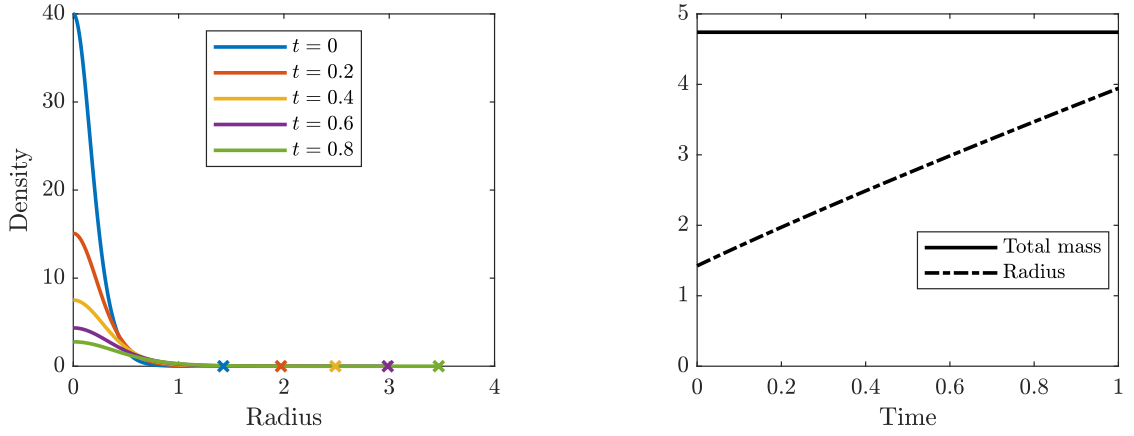


**Figure 3.5:** The pictures show the time evolution of a fluid ball with $\alpha = -1$, $\phi_1 = 2$, and $\rho_0^c = 40$. For clarity, crosses have been marked on the x-axis in the left picture to indicate where each curve ends, that is, they indicate the radius of the ball at each time step. When $\alpha = -1$, the critical value for $\phi_1$ is $\sqrt{2}$, so the ball will expand infinitely. The y-axis in in the right picture is not labeled because we have plotted both the total mass and the radius despite the different units.

# 4

# Static Self-Gravitating Elastic Bodies

This chapter is the elastic counterpart of Section 3.1 and we study static elastic bodies. The numerical results presented in this chapter relate to the first two objectives of the thesis.

Applying the Definition 4 of a strongly regular static self-gravitating elastic ball, the system (2.11) of static equilibrium becomes

$$a(\delta,\eta)\delta' = \frac{b(\delta,\eta)}{r}(\eta-\delta) - G\mathcal{K}\delta\frac{m}{r^2}, \tag{4.1a}$$

$$\eta' = -\frac{3}{r}(\eta-\delta), \tag{4.1b}$$

$$m' = 4\pi\mathcal{K}r^2\delta \tag{4.1c}$$

where

$$a(\delta,\eta) = \partial_\delta\widehat{p}_{\mathrm{rad}}(\delta,\eta), \quad b(\delta,\eta) = 2\frac{\widehat{p}_{\tan}(\delta,\eta)-\widehat{p}_{\mathrm{rad}}(\delta,\eta)}{\eta-\delta} + 3\partial_\eta\widehat{p}_{\mathrm{rad}}(\delta,\eta). \tag{4.2}$$

The solution depends on the constitutive functions used to close the system and are commonly given in terms of the Lamé material constants $\lambda$ and $\mu$. For example, iron has the Lamé parameter values $\lambda = 9.9\cdot10^5$ kg/cm$^2$ and $\mu = 7.8\cdot10^5$ kg/cm$^2$. They satisfy $\mu > 0$ and $(3\lambda+2\mu) > 0$, so when numerically investigating a material model one would have to search a large two-dimensional parameter space. To avoid this, the Lamé parameters can be replaced by the **bulk modulus**, $\kappa$, and the **Poisson ratio**, $\nu$, by letting

$$\kappa = \frac{3\lambda+2\mu}{3}, \quad \nu = \frac{\lambda}{2(\lambda+\mu)}. \tag{4.3}$$

Since $\kappa > 0$ appears only as a proportionality constant in the constitutive equations considered below, we only have to take $\nu$ into consideration when investigating the qualitative behaviour of solutions to system (4.1). Moreover, $\nu$ is dimensionless and the theoretical values $\nu$ can take on are restricted to $\nu \in (-1, 1/2)$ and most materials have a positive Poisson ratio [8]. This drastically simplifies numerical investigations.

The material models in this chapter are given in terms of their stored energy

functions $w$. Recall that the constitutive functions are then given by $\widehat{p}_{\mathrm{rad}}(\delta,\eta) = \delta^2\partial_\delta w(\delta,\eta)$ and $\widehat{p}_{\mathrm{tan}}(\delta,\eta) = \widehat{p}_{\mathrm{rad}}(\delta,\eta) + \frac{3}{2}\delta\eta\partial_\eta w(\delta,\eta)$.

**Definition 8.** *The inequality*

$$\frac{\widehat{p}_{\mathrm{tan}}(\delta,\eta) - \widehat{p}_{\mathrm{rad}}(\delta,\eta)}{\eta-\delta} > 0, \tag{4.4}$$

*on the elastic constitutive function $(\widehat{p}_{\mathrm{rad}}, \widehat{p}_{\mathrm{tan}})$ for spherically symmetric bodies is called the strong Baker-Ericksen inequality if it is satisfied for all $(\delta,\eta) \in \mathbb{R}^2$ and weak Baker-Ericksen inequality if it is satisfied for all $(\delta,\eta) \in \mathbb{R}^2 : \eta > \delta$.*

The Baker-Ericksen inequality is a physically motivated inequality that any physically relevant constitutive function should satisfy. It is proved in [2] that solutions to (4.1) satisfy $\eta(r) > \delta(r)$ for all $r > 0$, so it should also hold that $\widehat{p}_{\mathrm{tan}}(\delta,\eta) > \widehat{p}_{\mathrm{rad}}(\delta,\eta)$ for all $r > 0$. We will return to this inequality later in the chapter.

The so called **strict hyperbolicity condition**, $\partial_\delta\widehat{p}_{\mathrm{rad}}(\delta,\eta) > 0$, played a central role in the results proved in [2], so it is of interest to see what happens when it is violated. Since $\delta(0) = \eta(0) = \delta_c$, the hyperbolicity condition at the center is

$$\partial_\delta\widehat{p}_{\mathrm{rad}}(\delta_c,\delta_c) > 0. \tag{4.5}$$

For this reason we introduce the constant $\Delta_\flat$ such that (4.5) holds for $0 < \delta_c < \Delta_\flat$, $\partial_\delta\widehat{p}_{\mathrm{rad}}(\Delta_\flat,\Delta_\flat) = 0$, and $\partial_\delta\widehat{p}_{\mathrm{rad}}(\delta_c,\delta_c) < 0$ for $\delta_c > \Delta_\flat$. Such a constant exists for all elastic models considered in this chapter.

The following five sections present one material model each. They follow roughly the same outline. We first introduce the stored energy function for the model, and expressions for the the principal pressures. This is followed by the relevant results proved in [2] about the existence of solutions, and the problems left open. Lastly we present our numerical findings.

Since we are interested in the existence and qualitative behaviour of the solutions rather than quantitative ones, we plot the dimensionless pressures $\kappa^{-1}p_{\mathrm{rad}}$ and $\kappa^{-1}p_{\mathrm{tan}}$, and the dimensionless density $\delta = \mathcal{K}^{-1}\rho$.

## 4.1 Saint Venant-Kirchhoff materials

The Saint Venant-Kirchhoff material model is hyperelastic with stored energy function

$$\begin{aligned}\kappa^{-1}\widehat{w}_{\mathrm{SVK}}(\delta,\eta) = \eta^{-4/3}&\left(\frac{3(1-\nu)}{8(1+\nu)}\left(\frac{\delta}{\eta}\right)^{-4} + \frac{3\nu}{2(1+\nu)}\left(\frac{\delta}{\eta}\right)^{-2} + \frac{3}{4(1+\nu)}\right)\\ &+ \eta^{-2/3}\left(-\frac{3}{4}\left(\frac{\delta}{\eta}\right)^{-2} - \frac{3}{2}\right) + \frac{9}{8},\end{aligned}$$

which yields the principal pressures

$$\kappa^{-1}\widehat{p}_{\mathrm{rad}}(\delta,\eta) = \frac{3\eta^{2/3}\left(\delta^2\left(\eta^{2/3}(\nu+1)-2\nu\right)+\eta^2(\nu-1)\right)}{2\delta^3(\nu+1)},$$
$$\kappa^{-1}\widehat{p}_{\tan}(\delta,\eta) = \frac{3\left(\delta^2\left(\eta^{2/3}(\nu+1)-1\right)-\eta^2\nu\right)}{2\delta\eta^{4/3}(\nu+1)}.$$

At the center

$$\kappa^{-1}\widehat{p}_{\mathrm{rad}}(\delta_c,\delta_c) = \kappa^{-1}\widehat{p}_{\tan}(\delta_c,\delta_c) = \frac{3\left(\delta_c^{2/3}-1\right)}{2\delta_c^{1/3}},$$
$$\kappa^{-1}\partial_\delta\widehat{p}_{\mathrm{rad}}(\delta_c,\delta_c) = -\frac{3\left((1+\nu)\delta_c^{2/3}+\nu-3\right)}{2(\nu+1)\delta_c^{4/3}}.$$

It is clear that the pressures are positive at the center if and only if $\delta_c > 1$, and that the constant $\Delta_\flat$ is given by

$$\Delta_\flat = \left(\frac{3-\nu}{1+\nu}\right)^{3/2}.$$

The following theorem was proved in [2]:

**Theorem 3.** *When the elastic material is given by the Saint Venant-Kirchhoff model, the condition $\delta_c := \rho_c/\mathcal{K} > 1$ is necessary for the existence of regular static self-gravitating balls, while the condition $\delta_c < \Delta_\flat$ is necessary for the strict hyperbolicity condition (4.5) to be satisfied at the center. When $1 < \delta_c < \Delta_\flat$ there exists a unique strongly regular static self-gravitating ball with central density $\rho(0) = \rho_c$. Moreover $\partial_\delta\widehat{p}_{\mathrm{rad}}(\delta_c,\delta_c) > 0$ and*

$$\partial_\delta\widehat{p}_{\mathrm{rad}}(\delta(r),\eta(r)) > 0, \quad \rho(r) < \rho_c, \quad \frac{4\pi}{3}\max(\rho(r),\mathcal{K})r^3 < m(r) < \frac{4\pi}{3}\rho_c r^3$$

*hold for all $r \in (0,R]$, where $R > 0$ is the radius of the ball.*

We are interested in the following question.

**Open Problem 1.** *Can finite radius elastic balls exist in the Saint Venant-Kirchhoff material model when the strict hyperbolicity condition is violated at the center?*

We have found numerical evidence suggesting that regardless of $\nu$, finite radius solutions cannot be constructed when $\delta_c \geq \Delta_\flat$. The density and pressures blow up almost immediately, see Figure 4.1.

Note also that in Figure 4.1a the radial pressure is at times larger than the tangential pressure. This would mean that it violates the Baker-Ericksen inequality (4.4). This only happened for central densities very close to $\Delta_\flat$.

Mass-radius diagrams were constructed for three different Poisson ratios $\nu$, see Figure 4.2. We see that for small $\nu$, the curve spirals back around for large central densities. However, it does not seem to continue spiraling, but rather converge monotonically to a point.

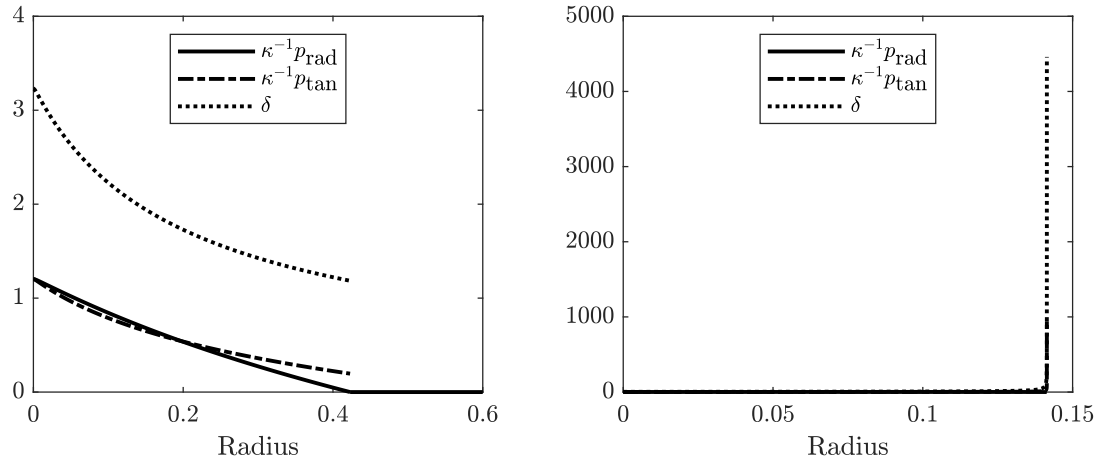


**(a)** $\delta_c = 0.99\Delta_\flat$. **(b)** $\delta_c = 1.01\Delta_\flat$.

**Figure 4.1:** Elastic balls constructed in the Saint Venant-Kirchoff material model with Poisson ratio $\nu = 0.25$ for center datum close to $\Delta_\flat$ ($\approx 3.26$).

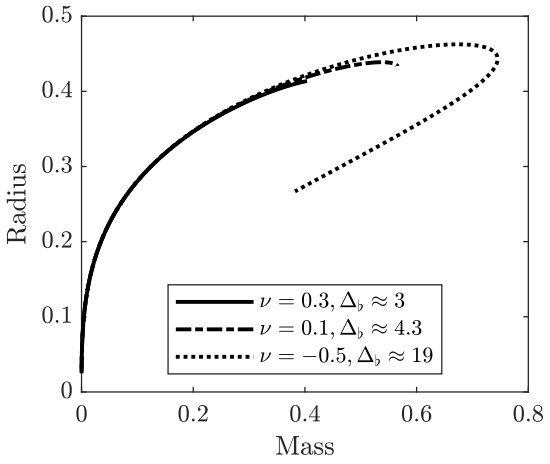


**Figure 4.2:** Mass-radius diagram for the Saint Venant-Kirchhoff material model for different values of $\nu$ with center datum in the interval $\delta_c \in (1, \Delta_\flat)$.

## 4.2 Quasi-linear John materials

Quasi-linear John materials are hyperelastic with stored energy function

$$\begin{aligned}\kappa^{-1}\widehat{w}_{\mathrm{John}}(\delta,\eta) = \eta^{-1}&\left(-\frac{3(1-2\nu)}{1+\nu}\left(\frac{\delta}{\eta}\right)^{-1}\right)\\ &+\eta^{-2/3}\left(\frac{3(1-\nu)}{2(1+\nu)}\left(\frac{\delta}{\eta}\right)^{-2}+\frac{6(1-\nu)}{1+\nu}\left(\frac{\delta}{\eta}\right)^{-1}+\frac{6(1-\nu)}{1+\nu}\right)\\ &+\eta^{-1/3}\left(-\frac{3(2-\nu)}{1+\nu}\left(\frac{\delta}{\eta}\right)^{-1}-\frac{6(2-\nu)}{1+\nu}\right)+\frac{3(5-\nu)}{2(1+\nu)},\end{aligned}$$

which yields the principal pressures

$$\kappa^{-1}\widehat{p}_{\rm rad}(\delta,\eta) = \frac{3\left(\delta\left(-\eta^{2/3}(\nu-2)+2\eta^{1/3}(\nu-1)-2\nu+1\right)+\eta^{4/3}(\nu-1)\right)}{\delta(\nu+1)},$$
$$\kappa^{-1}\widehat{p}_{\rm tan}(\delta,\eta) = \frac{3\left(-\delta\eta^{1/3}(\nu-2)+2\delta(\nu-1)+\eta^{2/3}(1-2\nu)+\eta(\nu-1)\right)}{\eta^{2/3}(\nu+1)}.$$

At the center

$$\kappa^{-1}\widehat{p}_{\rm rad}(\delta_c,\delta_c) = \kappa^{-1}\widehat{p}_{\rm tan}(\delta_c,\delta_c) = \frac{3\left({\delta_c}^{1/3}-1\right)\left((2-\nu){\delta_c}^{1/3}+2\nu-1\right)}{\nu+1},$$
$$\kappa^{-1}\partial_\delta\widehat{p}_{\rm rad}(\delta_c,\delta_c) = -\frac{3(\nu-1)}{(\nu+1)\delta_c^{2/3}}.$$

It is clear that the pressures are positive at the center if and only if $\delta_c > 1$ or $0 < \delta_c < \Delta_*$, where

$$\Delta_* = \left(\frac{1-2\nu}{2-\nu}\right)^3 < 1,$$

and that the constant $\Delta_\flat$ is given by $\Delta_\flat = \infty$.

The following theorem was proved in [2]:

**Theorem 4.** *When the elastic material is given by the John model, for all $\delta_c := \rho_c/\mathcal{K} > 1$ there exists a unique strongly regular static self-gravitating ball with central density $\rho(0) = \rho_c$. Moreover $\partial_\delta\widehat{p}_{\rm rad}(\delta_c,\delta_c) > 0$ and*

$$\partial_\delta\widehat{p}_{\rm rad}(\delta(r),\eta(r)) > 0, \quad \rho(r) < \rho_c, \quad \frac{4\pi}{3}\max(\rho(r),\mathcal{K})r^3 < m(r) < \frac{4\pi}{3}\rho_c r^3$$

*hold for all $r \in (0,R]$, where $R > 0$ is the radius of the ball.*

We are interested in the following question.

**Open Problem 2.** *Is $\delta_c > 1$ a necessary condition or can finite radius elastic balls exist in the quasi-linear John material model when $0 < \delta_c < \Delta_*$?*

In our numerical investigations we have found evidence suggesting the existence of a constant $\Delta_\circ$, dependent on $\nu$, such that finite radius balls do exist when $\delta_c \in [\Delta_\circ, \Delta_*)$ but not when $\delta_c < \Delta_\circ$, see Figure 4.3. We have not a found a closed expression for $\Delta_\circ$, but Figure 4.4 shows where in the $(\nu,\delta_c)$-plane finite radius balls could be constructed numerically.

An interesting property of these solutions is that the tangential pressure is increasing with the radius rather than decreasing, which seems to be the case for solutions with center datum $\delta_c > 1$, see Figure 4.5.

Mass-radius diagrams were constructed both for $\delta_c \in [\Delta_\circ, \Delta_*)$ and $\delta_c > 1$, where the numerical approximations of $\Delta_\circ$ were used, see Figure 4.6. In Figure 4.6b the curves eventually turns back around for large central densities, but rather than continue spiraling they seem to converge monotonically.

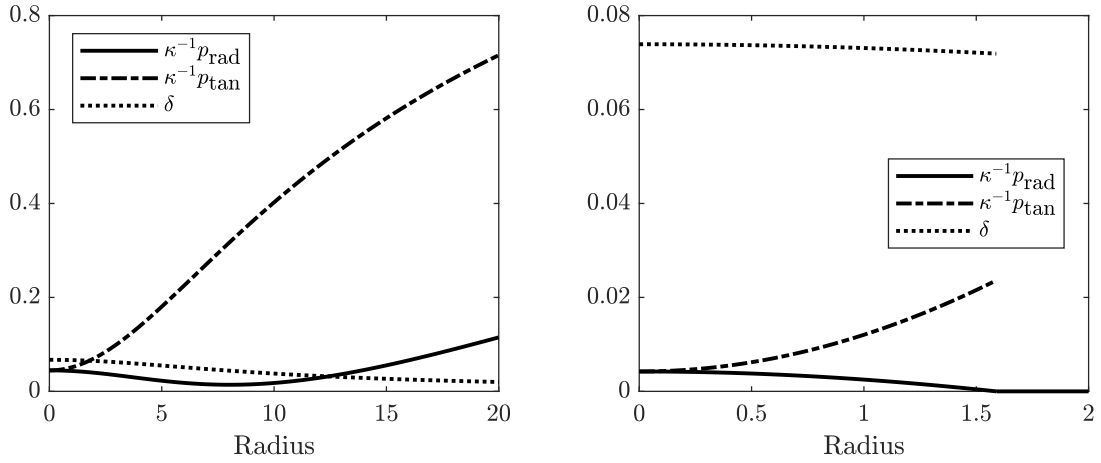


**(a)** $\delta_c = 0.90\Delta_*$. **(b)** $\delta_c = 0.99\Delta_*$.

**Figure 4.3:** Elastic balls constructed in the quasi-linear John material model with Poisson ratio $\nu = 0.1$ for center datum smaller than $\Delta_*$ ($\approx 0.0746$). Only in (b) does the ball have finite radius. There seems to exist a $\Delta_\circ$ such that when $\delta_c = \Delta_\circ$, $\kappa^{-1}p_{\mathrm{rad}}$ just about touches the x-axis.

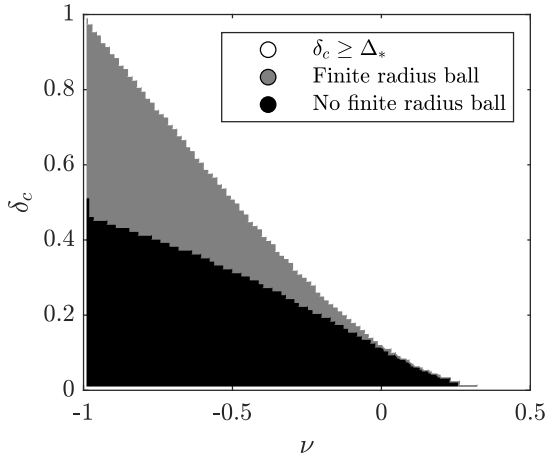


**Figure 4.4:** The gray region indicates where finite radius balls have been found numerically in the quasi-linear John model for $\delta_c \in (0, \Delta_*)$. The border between the black and gray regions approximates the proposed $\Delta_\circ(\nu)$.

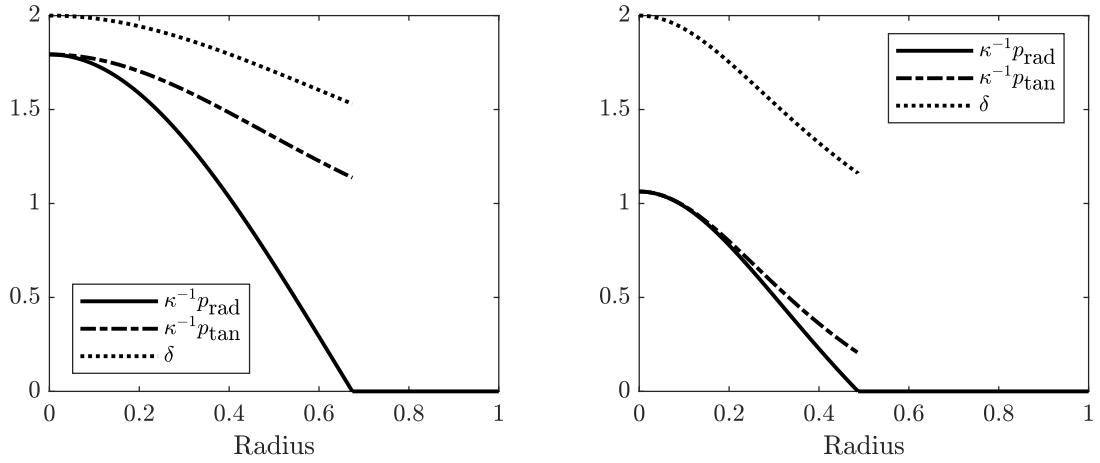


**(a)** $\nu = -0.5$. **(b)** $\nu = 0.25$.

**Figure 4.5:** Elastic balls constructed in the quasi-linear John material model with center datum $\delta_c = 2$. The tangential pressure decreases with the radius as opposed to when $\delta_c < 1$, see Figure 4.3.

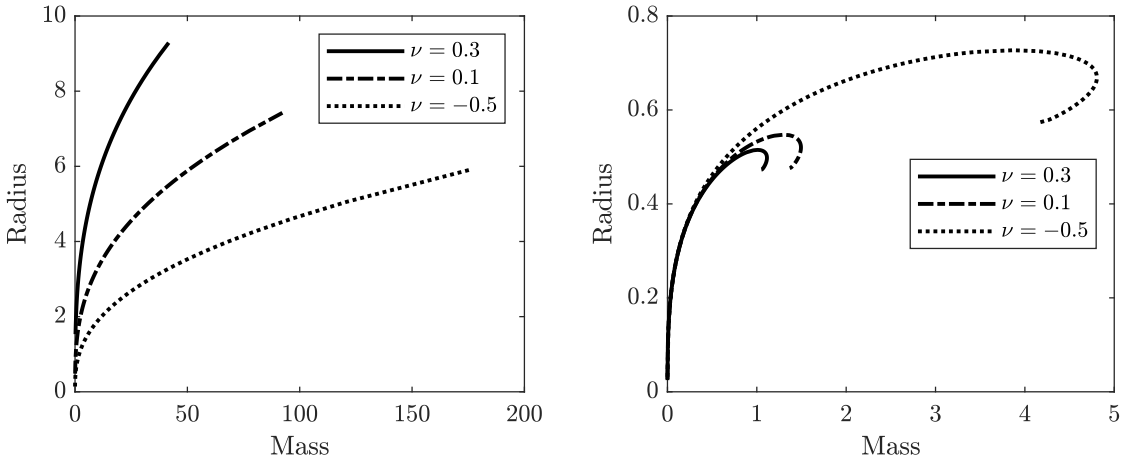


**(a)** $\delta_c \in [\Delta_\circ, \Delta_*)$. **(b)** $\delta_c > 1$.

**Figure 4.6:** Mass-radius diagrams for the quasi-linear John material model for different values of $\nu$. Solutions closer to the origin correspond to solutions with center datum closer to $\Delta_*$ in (a) and center datum closer to 1 in (b).

## 4.3 Hadamard materials

Hadamard materials are hyperelastic materials with stored energy function

$$\kappa^{-1}\widehat{w}_{\mathrm{Had}}(\delta,\eta) = \eta^{-4/3}\left(\frac{3}{2(1+\nu)}\left(\frac{\delta}{\eta}\right)^{-2} + \frac{3}{4(1+\nu)}\right) - \eta^{-1}\left(\frac{3(1-\nu)}{1+\nu}\left(\frac{\delta}{\eta}\right)^{-1}\right) + \eta^{-2/3}\left(-\frac{3\nu}{2(1+\nu)}\left(\frac{\delta}{\eta}\right)^{-2} - \frac{3\nu}{1+\nu}\right) + \frac{3(1+2\nu)}{4(1+\nu)},$$

where $\nu$ is now assumed to be positive. This yields the principal pressures

$$\kappa^{-1}\widehat{p}_{\mathrm{rad}}(\delta,\eta) = \frac{3\left(-\delta\nu + \delta + \eta^{4/3}\nu - \eta^{2/3}\right)}{\delta(\nu+1)},$$
$$\kappa^{-1}\widehat{p}_{\mathrm{tan}}(\delta,\eta) = \frac{3\left(\delta^2\left(2\eta^{2/3}\nu - 1\right) - 2\delta\eta^{4/3}(\nu-1) - \eta^2\right)}{2\delta\eta^{4/3}(\nu+1)},$$

and at the center we have

$$\kappa^{-1}\widehat{p}_{\mathrm{rad}}(\delta_c,\delta_c) = \kappa^{-1}\widehat{p}_{\mathrm{rad}}(\delta_c,\delta_c) = \frac{3\left({\delta_c}^{1/3} - 1\right)\left(\nu{\delta_c}^{1/3} + 1\right)}{(\nu+1){\delta_c}^{1/3}},$$
$$\kappa^{-1}\partial_\delta\widehat{p}_{\mathrm{rad}}(\delta_c,\delta_c) = \frac{3\left(1 - \nu\delta_c^{2/3}\right)}{(\nu+1)\delta_c^{4/3}}.$$

It is clear that the pressures are positive at the center if and only if $\delta_c > 1$, and the constant $\Delta_\flat$ is given by

$$\Delta_\flat = \left(\frac{1}{\nu}\right)^{3/2}.$$

The following theorem has been proved in [2]:

**Theorem 5.** *When the elastic material is given by the Hadamard model, the condition $\delta_c := \rho_c/\mathcal{K} > 1$ is necessary for the existence of regular static self-gravitating balls. For*

$$1 < \delta_c < \left(\frac{1}{2\nu}\right)^{3/2} = \Delta_\sharp$$

*there exists a unique strongly regular static self-gravitating ball with central density $\rho(0) = \rho_c$. Moreover $\partial_\delta\widehat{p}_{\mathrm{rad}}(\delta_c,\delta_c) > 0$ and*

$$\partial_\delta\widehat{p}_{\mathrm{rad}}(\delta(r),\eta(r)) > 0, \quad \rho(r) < \rho_c, \quad \frac{4\pi}{3}\max(\rho(r),\mathcal{K})r^3 < m(r) < \frac{4\pi}{3}\rho_c r^3$$

*hold for all $r \in (0,R]$, where $R > 0$ is the radius of the ball.*

We are interested in the following question.

**Open Problem 3.** *Is the sufficient bound $\delta_c < \Delta_\sharp$ in Theorem 5 necessary or can it be replaced by the weaker bound $\delta_c < \Delta_\flat$?*

In our numerical investigations we have found evidence suggesting that the bound

indeed can be replaced. Figure 4.7 shows finite radius balls with center datum both smaller than and larger than $\Delta_\sharp$. Furthermore, finite radius solutions seem to exist

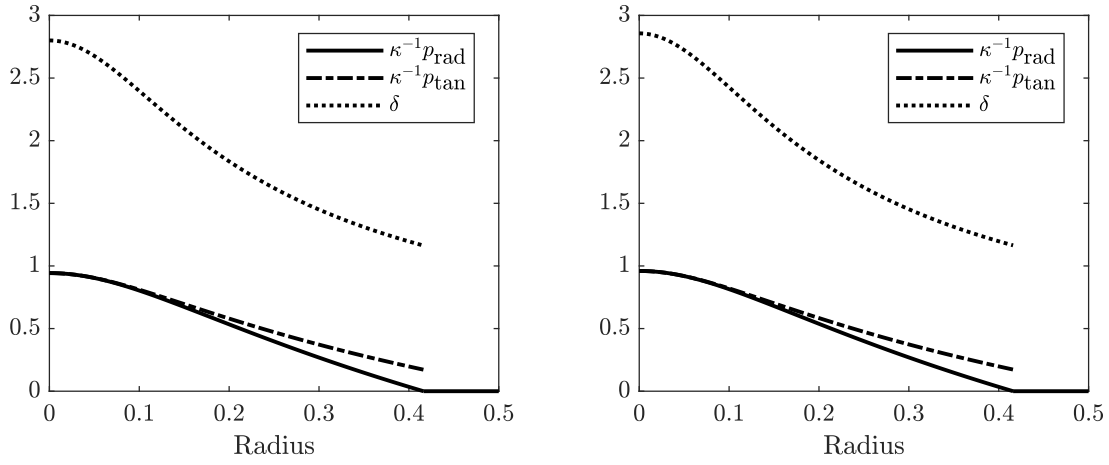


**(a)** $\delta_c = 0.99\Delta_\sharp$. **(b)** $\delta_c = 1.01\Delta_\sharp$.

**Figure 4.7:** Elastic balls constructed in the Hadamard material model with Poisson ratio $\nu = 0.25$ for center datum close to $\Delta_\sharp$ ($\approx 2.83$).

for center datum in the entire interval from $\Delta_\sharp$ up to $\Delta_\flat$, but not for $\delta_c \geq \Delta_\flat$, see Figure 4.8. When $\delta_c \geq \Delta_\flat$, the hyperbolicity condition is violated at the center and the numerical solutions in Figure 4.8b blows up similarly to how they did in the Saint Venant-Kirchhoff model.

Another similarity to the Saint Venant-Kirchhoff model is that the Baker-Ericksen inequality seems to be violated in Figure 4.8a since the radial pressure is sometimes larger than the tangential pressure.

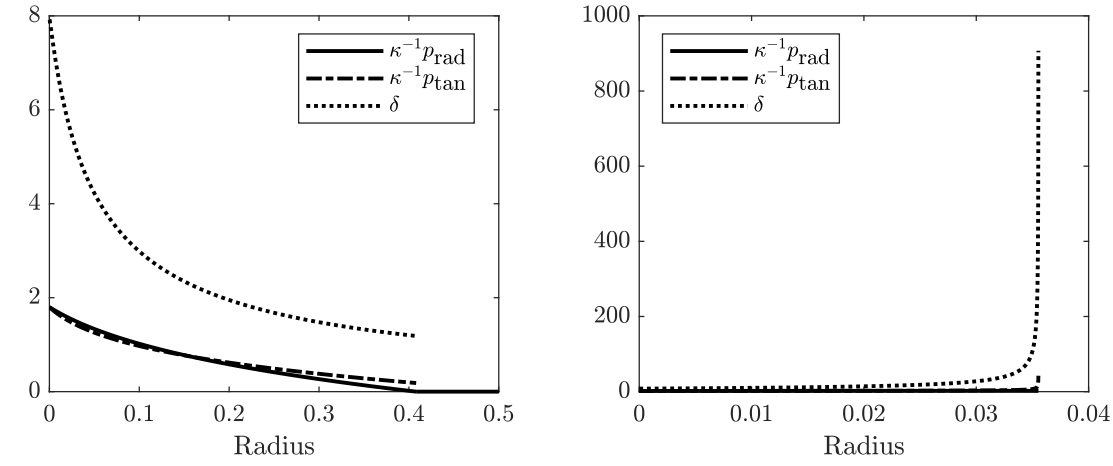


**(a)** $\delta_c = 0.99\Delta_\flat$. **(b)** $\delta_c = 1.01\Delta_\flat$.

**Figure 4.8:** Elastic balls constructed in the Hadamard material model with Poisson ratio $\nu = 0.25$ for center datum close to $\Delta_\flat$ ($\approx 8$).

Mass-radius diagrams were constructed for center datum in the interval $\delta_c \in (1, \Delta_\flat)$, see Figure 4.9. We see that for small $\nu$, the curve spirals back around for large central densities. However, it seems to eventually converge monotonically to a point rather than continue spiraling.

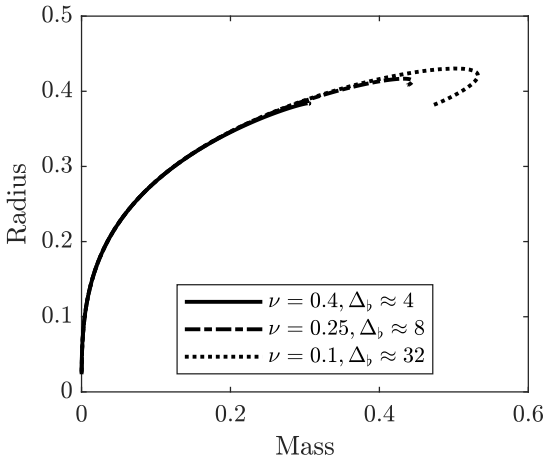


**Figure 4.9:** Mass-radius diagrams for the Hadamard material model for different values of $\nu$ with center datum in the interval $\delta_c \in (1, \Delta_\flat)$.

## 4.4 Quasi-linear Signorini materials

Quasi-linear Signorini materials are hyperelastic with stored energy function

$$\kappa^{-1}\widehat{w}_{\mathrm{Sig}}(\delta,\eta) = \frac{3(5+8\nu)}{16(1+\nu)}\eta^{-1}\left(\frac{\delta}{\eta}\right)^{-1} + \eta^{-\frac{1}{3}}\left(-\frac{3(1+4\nu)}{4(1+\nu)}\left(\frac{\delta}{\eta}\right)^{-1} - \frac{3(1+4\nu)}{8(1+\nu)}\left(\frac{\delta}{\eta}\right)\right)$$
$$+ \eta^{\frac{1}{3}}\left(\frac{3}{4(1+\nu)}\left(\frac{\delta}{\eta}\right)^{-1} + \frac{3}{4(1+\nu)}\left(\frac{\delta}{\eta}\right) + \frac{3}{16(1+\nu)}\left(\frac{\delta}{\eta}\right)^{3}\right) - \frac{3(1-2\nu)}{2(1+\nu)},$$

which yields the principal pressures

$$\kappa^{-1}\widehat{p}_{\mathrm{rad}}(\delta,\eta) = \frac{3\left(2\delta^2\eta^{4/3}\left(2\eta^{2/3}-4\nu-1\right)+3\delta^4+\eta^{8/3}\left(4\eta^{2/3}(4\nu+1)-4\eta^{4/3}-8\nu-5\right)\right)}{16\eta^{8/3}(\nu+1)},$$

$$\kappa^{-1}\widehat{p}_{\tan}(\delta,\eta) = \frac{3\left(2\delta^2\eta^{4/3}(4\nu+1)-\delta^4-\eta^{8/3}\left(-4\eta^{4/3}+8\nu+5\right)\right)}{16\eta^{8/3}(\nu+1)}.$$

At the center

$$\kappa^{-1}\widehat{p}_{\mathrm{rad}}(\delta_c,\delta_c) = \kappa^{-1}\widehat{p}_{\tan}(\delta_c,\delta_c) = \frac{3\left(\delta_c^{2/3}-1\right)\left(3\delta_c^{2/3}+8\nu+5\right)}{16(\nu+1)},$$

$$\kappa^{-1}\partial_\delta\widehat{p}_{\mathrm{rad}}(\delta_c,\delta_c) = \frac{3\left(5\delta_c^{2/3}-4\nu-1\right)}{4(\nu+1){\delta_c}^{1/3}}.$$

The pressures are positive at the center if and only if $\delta_c > 1$ or, when $\nu \in (-1, -5/8)$, $0 < \delta_c < \Delta_*$, where

$$\Delta_* = \left(\frac{-5 - 8\nu}{3}\right)^{3/2} < 1.$$

Furthermore, the constant $\Delta_\flat$ is given by $\Delta_\flat = \infty$.

*Remark.* The hyperbolicity condition is violated at the center if $\delta_c < ((4\nu+1)/5)^{3/2}$ but this only happens for invalid combinations of $\delta_c$ and $\nu$, i.e., where the principal pressures are negative at the center.

The results in [2] do not cover the quasi-linear Signorini materials, so we are interested in the following questions.

**Open Problem 4.** *Do finite radius elastic balls exist in the quasi-linear Signorini material model when (a) $\delta_c > 1$, (b) $0 < \delta_c < \Delta_*$?*

Regarding question (a) we were able to numerically construct finite radius balls for every combination of $\nu \in (-1, 1/2)$ and $\delta_c > 1$ that we tried, see Figure 4.10 for examples. Regarding question (b), we found numerical evidence suggesting the existence of a constant $\Delta_\circ$, dependent on $\nu \in (-1, -5/8)$, such that finite radius balls do exist when $\delta_c \in [\Delta_\circ, \Delta_*)$ but not when $\delta_c < \Delta_\circ$, see Figure 4.11. We have not been able to derive a closed expression for $\Delta_\circ$, but Figure 4.12 shows where in the $(\nu, \delta_c)$-plane finite radius balls could be constructed numerically.

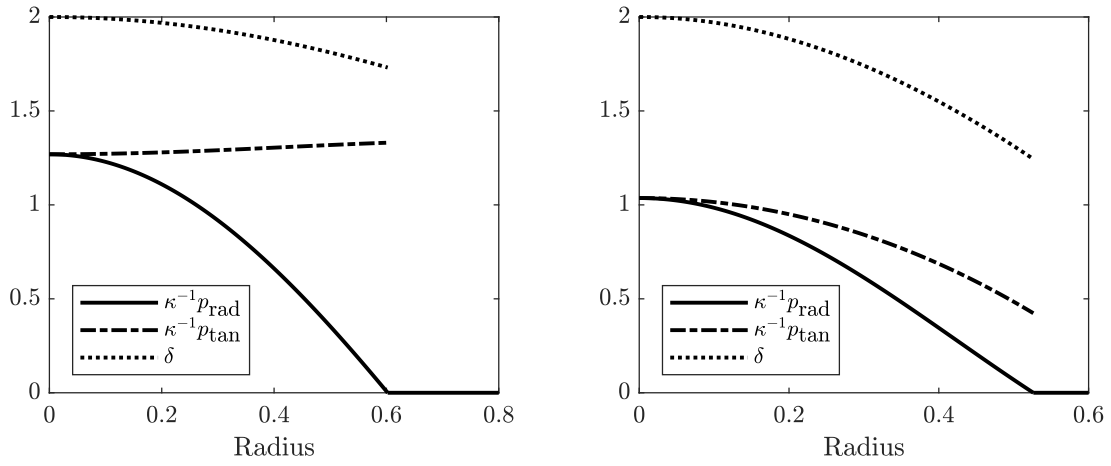


**(a)** $\nu = -0.5$. **(b)** $\nu = 0.25$.

**Figure 4.10:** Elastic balls constructed in the quasi-linear Signorini material model with center datum $\delta_c = 2$.

Mass-radius diagrams were constructed both for $\delta_c \in [\Delta_\circ, \Delta_*)$ and $\delta_c > 1$, where the numerical approximations of $\Delta_\circ$ were used, see Figure 4.13.

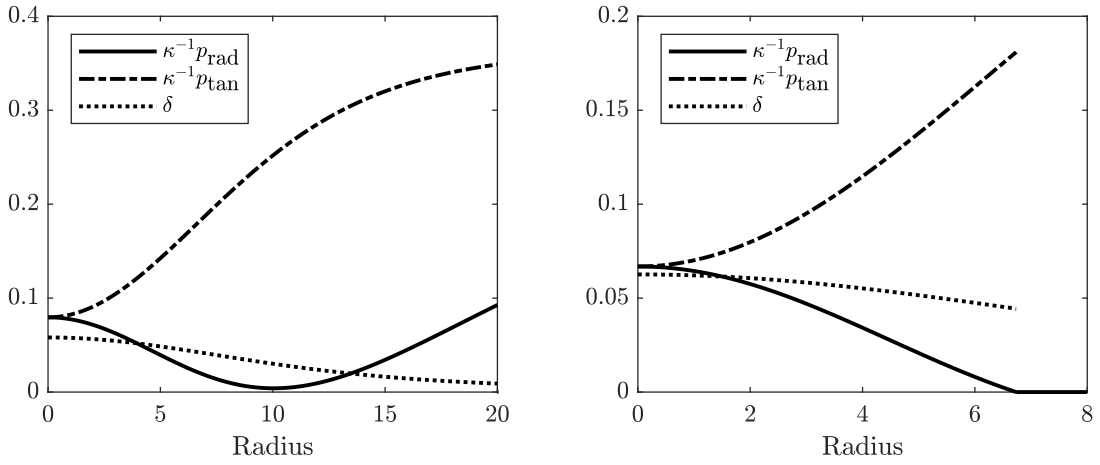


**(a)** $\delta_c = 0.65\Delta_*$. **(b)** $\delta_c = 0.70\Delta_*$.

**Figure 4.11:** Elastic balls constructed in the quasi-linear Signorini material model with Poisson ratio $\nu = -0.7$ for center datum smaller than $\Delta_*$ ($\approx 0.0894$). Only in (b) does the ball have finite radius. There seems to exist a $\Delta_\circ$ such that when $\delta_c = \Delta_\circ$, $\kappa^{-1}p_{\text{rad}}$ just about touches the x-axis.

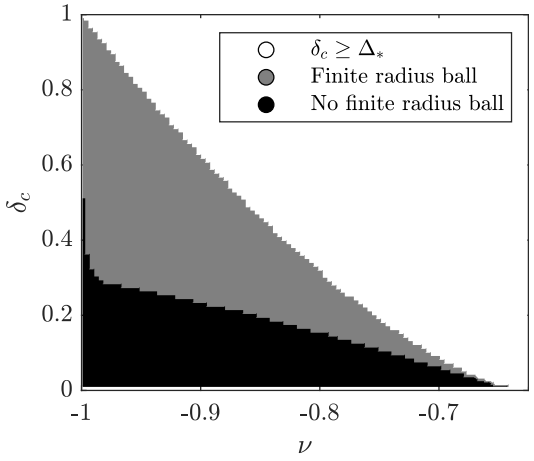


**Figure 4.12:** The gray region indicates where finite radius balls have been found numerically in the quasi-linear Signorini model for $\delta_c \in (0, \Delta_*)$. The border between the black and gray regions approximates the proposed $\Delta_\circ(\nu)$.

## 4.5 Polytropic elastic materials

The previous material models are phenomenological and work well for engineering purposes on Earth, but from an astrophysical and mathematical point of view they have some strange and unwanted properties. For this reason a new two-parameter family of stored energy functions was recently introduced in [4] with the purpose of generalizing the polytropic fluid model to elastic materials. It is hyperelastic and

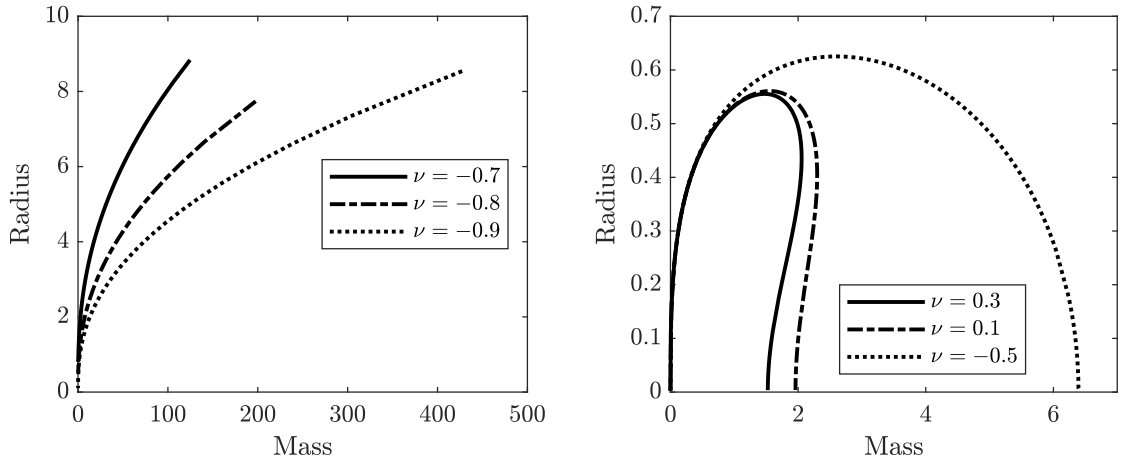


**(a)** $\delta_c \in [\Delta_\circ, \Delta_*)$. **(b)** $\delta_c > 1$ .

**Figure 4.13:** Mass-radius diagrams for the quasi-linear Signorini material model for different values of $\nu$. Solutions closer to the origin correspond to solutions with center datum closer to $\Delta_*$ in (a) and center datum closer to 1 in (b).

the stored energy function is given by

$$\kappa^{-1}\widehat{w}(\delta,\eta) = \frac{1}{1+\gamma}\delta^{-1} - \frac{1}{\gamma} + \eta^{\gamma}\left(\frac{3(1-\nu)}{\beta(1+\beta)(1+\nu)}\left(\frac{\delta}{\eta}\right)^{\beta} + \left(\frac{3(1-\nu)}{(1+\beta)(1+\nu)} - \frac{1}{1+\gamma}\right)\left(\frac{\delta}{\eta}\right)^{-1} + \frac{1}{\gamma} - \frac{3(1-\nu)}{\beta(1+\nu)}\right) \tag{4.6}$$

where $\beta, \gamma \neq -1, 0$. Keep in mind that $\beta$ and $\gamma$ are not material parameters but model parameters. When $\nu = 1/2$ and $\beta = \gamma$ the model reduces to a fluid model. Under certain mild conditions, this is the unique model that satisfies the scale invariance property

$$\varepsilon^{-\gamma} a(\varepsilon\delta, \varepsilon\eta) = a(\delta,\eta), \quad \varepsilon^{-\gamma} b(\varepsilon\delta, \varepsilon\eta) = b(\delta,\eta), \tag{4.7}$$

for all $\varepsilon > 0$, where $a, b$ are defined in (4.2) [4]. This property in used later in Chapter 5.

At the center we have

$$\kappa^{-1}\widehat{p}_{\mathrm{rad}}(\delta_c,\delta_c) = \kappa^{-1}\widehat{p}_{\mathrm{tan}}(\delta_c,\delta_c) = \frac{\delta_c^{1+\gamma}-1}{1+\gamma}$$
$$\kappa^{-1}\partial_\delta\widehat{p}_{\mathrm{rad}}(\delta_c,\delta_c) = \frac{3\delta_c^{\gamma}(1-\nu)}{1+\nu}.$$

The principal pressures are positive at the center if and only if $\delta_c > 1$, and the hyperbolicity condition is not violated for any $\delta_c > 0$, that is, $\Delta_\flat = \infty$. The latter was in fact a required condition when constructing the model itself.

In [4] a differentiation is made between two types of solutions:

**Definition 9.** *Let $\mathfrak{B}$ be a strongly regular static self-gravitating elastic ball obtained by truncating a strongly regular solution of* (4.1) *with maximal interval of existence* $[0, R_{\max})$. *If $R_{\max} = \infty$, $\mathfrak{B}$ is of type* I *while if $R_{\max} < \infty$, $\mathfrak{B}$ is of type* II.

The characterization of type I and type II solutions is still under investigation, but we have been able to numerically construct balls of both types, see Figure 4.14. Even when $\delta$ and $\eta$ only exist locally, a finite radius ball can be obtained by truncating the solution. In fact, this is proved in [4] to always be the case when the weak Baker-Ericksen inequality is satisfied. The range of the parameters $\beta$ and $\gamma$ where it is satisfied is derived in [4]. It is for example satisfied when $\beta < \gamma$.

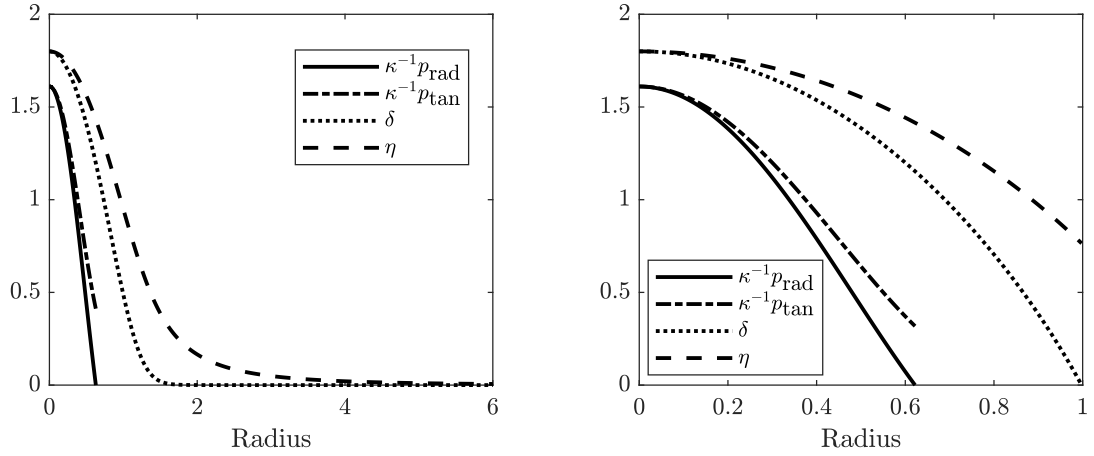


**(a)** $\beta = -0.5$. **(b)** $\beta = 1$.

**Figure 4.14:** Solutions of type I (left) and type II (right) to (4.1) in the polytropic elastic model with $\gamma = 2$, Poisson ratio $\nu = 0.4$, and center datum $\delta_c = 1.8$.

Mass-radius diagrams were constructed for numerous combinations of $\beta, \gamma$ and $\nu$. For $\gamma > 0$ they appeared to be only very slightly dependent on $\beta$ and $\nu$. Three main types of shapes were detected, one for $\gamma = 1/3$, one for $0 < \gamma < 1/3$, and one for $\gamma > 1/3$, see Figure 4.15.

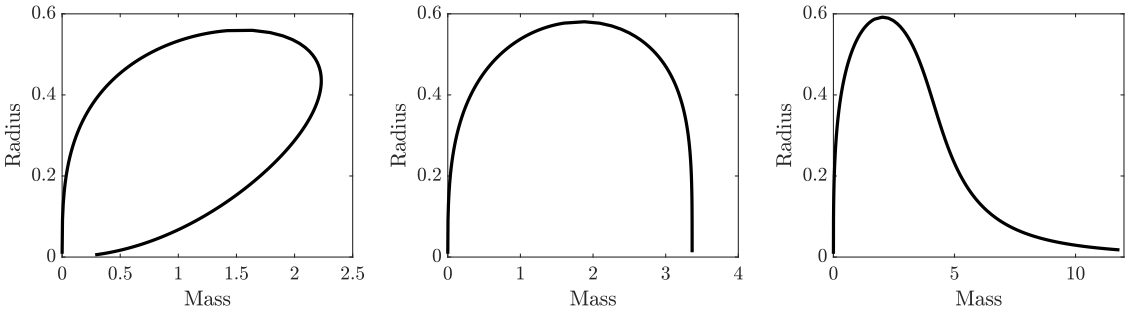


**(a)** $\gamma = 0.2$. **(b)** $\gamma = 1/3$. **(c)** $\gamma = 0.4$.

**Figure 4.15:** Mass-radius diagrams for polytropic elastic balls with $\beta = 0.5$ and Poisson ratio $\nu = 0.25$.

With $\gamma < 0$ there seemed to be two different cases, $\nu < 0$ and $\nu > 0$. For $\nu < 0$ the shapes of the mass-radius diagrams were similar to that of Figure 4.15a, and again seemed to be almost independent of $\beta$. For $\gamma < 0$ and $\nu > 0$ on the other hand there was no such clear pattern, and the shape depended on all three parameters. Some mass-radius diagrams were similar to Figure 4.15a while others were of a spiral shape, see Figure 4.16.

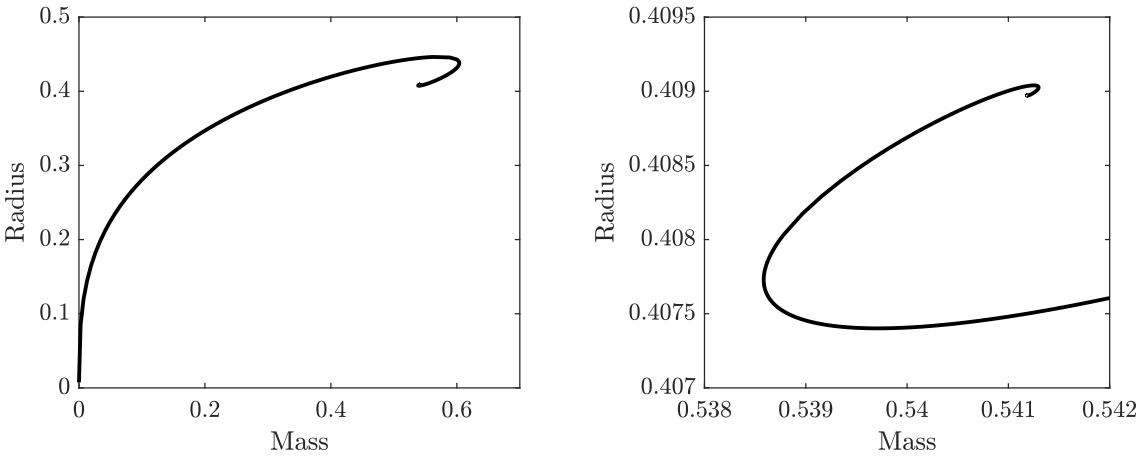


**Figure 4.16:** Mass-radius diagram for the polytropic elastic material model with $\beta = -0.8, \gamma = -0.75$ and Poisson ratio $\nu = 0.4$. The picture on the right is a magnification of the spiral in the picture on the left.

## 4.6 Shells and multi-bodies

Unlike in fluids, where the radial pressure is always decreasing with the radius, the radial pressure in elastic bodies can vanish in two points and thus form a shell with a vacuum core. Shell solutions are important as they can be used for instance to model crusts of celestial bodies.

**Definition 10.** *A (strongly regular) static self-gravitating shell of matter with* **inner radius** $R_{\text{in}} > 0$ *and* **outer radius** $R_{\text{out}} > R_{\text{in}}$ *is a triple* $(\rho, p_{\text{rad}}, p_{\text{tan}})$ *such that* $\Omega := \text{Int}\{r > 0 : \rho(r) > 0\} = (R_{\text{in}}, R_{\text{out}})$ *and*

*(i)* $(\rho, p_{\text{rad}}, p_{\text{tan}}) \in C^1([R_{\text{in}}, R_{\text{out}}])$ *satisfy* (2.11) *for* $r \in (R_{\text{in}}, R_{\text{out}})$,

*(ii)* $p_{\text{rad}}(r), p_{\text{tan}}(r)$ *are positive for* $r \in (R_{\text{in}}, R_{\text{out}})$,

*(iii)* $p_{\text{rad}}(R_{\text{in}}) = p_{\text{rad}}(R_{\text{out}}) = 0$,

*(v)* $\rho(r) = p_{\text{tan}}(r) = p_{\text{tan}}(r) = 0$, *for* $r \notin [R_{\text{in}}, R_{\text{out}}]$,

*If there exists an elastic constitutive function* $(\widehat{p}_{\text{rad}}, \widehat{p}_{\text{tan}})$ *satisfying* (2.17), (2.18) *and* (2.19) *such that*

$$p_{\text{rad}}(r) = \widehat{p}_{\text{rad}}(\delta(r), \eta(r)), \quad p_{\text{tan}}(r) = \widehat{p}_{\text{tan}}(\delta(r), \eta(r)),$$

*where*

$$\delta(r) = \frac{\rho(r)}{\mathcal{K}}, \quad \eta(r) = \left(\frac{\mathcal{S}}{r}\right)^3 + \frac{m_{\text{shell}}(r)}{\frac{4\pi}{3}\mathcal{K}r^3}, \quad m_{\text{shell}}(r) = 4\pi \int_{R_{\text{in}}}^{r} \rho(s)s^2\, ds \tag{4.8}$$

*for $r \in (R_{\text{in}}, R_{\text{out}})$, then we say that the shell is made of elastic matter and that it has reference density $\mathcal{K} > 0$ and reference inner radius $\mathcal{S} > 0$.*

To numerically construct an elastic shell one must:

1. Choose an inner radius $R_{\text{in}}$, which fixes $\eta_{\text{in}} = (\mathcal{S}/R_{\text{in}})^3$.
2. Determine $\delta_{\text{in}} = \delta(R_{\text{in}})$ by solving for (a positive) solution to $\widehat{p}_{\text{rad}}(\delta_{\text{in}}, \eta_{\text{in}}) = 0$.
3. Check that $\widehat{p}_{\text{tan}}(\delta_{\text{in}}, \eta_{\text{in}}) \geq 0$ and that $\frac{d}{dr}\widehat{p}_{\text{rad}}(\delta_{\text{in}}, \eta_{\text{in}}) > 0$. If not, the chosen $R_{\text{in}}$ is not feasible.
4. Integrate (4.1) up to the first radius $R_{\text{out}} > R_{\text{in}}$ at which the radial pressure vanishes.

A two-body configuration can be constructed in a similar way. First, construct either a ball or shell with (outer) radius $R_1$. Then apply the algorithm above starting at some $R_2 > R_1$ where the radial pressure is zero and integrate (4.1) up to where the radial pressure vanishes again. This method can be repeated to construct multi-body configurations.

The existence of shells and multi-bodies in the polytropic elastic model was not proved in [4] so we want to investigate the following.

**Open Problem 5.** *Do static self-gravitating shells and multi-bodies of matter exist in the polytropic elastic material model?*

In our numerical investigation we have successfully constructed numerous shells and multi-bodies, see Figure 4.17 for an example of a shell. Figure 4.18 shows a three-body configuration where the outermost shell is a different material than the two inner bodies.

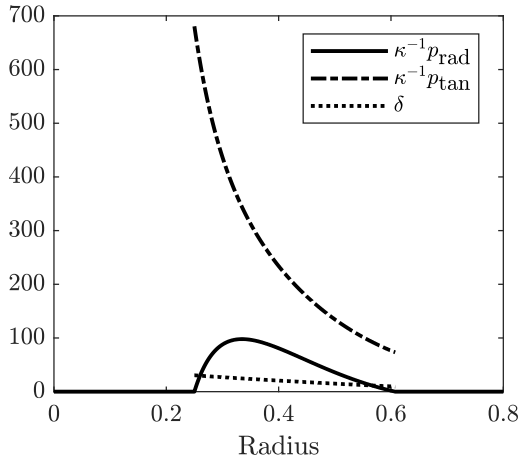


**Figure 4.17:** Shell constructed in the polytropic elastic material model with parameters $\beta = 0.8$ and $\gamma = 0.9$, Poisson ratio $\nu = 0.4$, reference inner radius $\mathcal{S} = 1$.

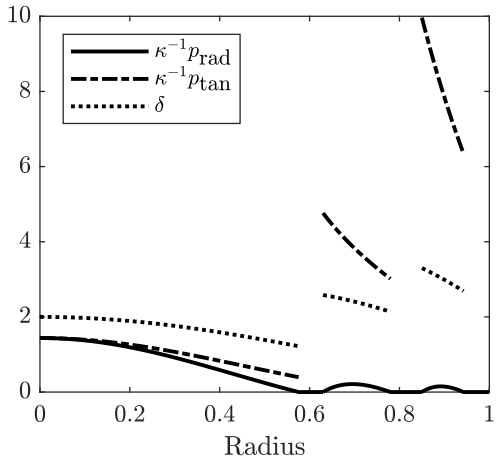


**Figure 4.18:** Multibody solution constructed in the polytropic elastic material model with parameters $\beta = 0.8$ and $\gamma = 0.9$, Poisson ratio $\nu_1 = 0.3$ for the ball and inner shell and $\nu_2 = 0.49$ for the outer shell, and reference inner radius $\mathcal{S}_1 = 1$ for the inner shell and $\mathcal{S}_2 = 2$ for the outer shell.

# 5

# Time-Dependent Self-Gravitating Elastic Balls

We now return to the Cauchy-Poisson system describing matter balls in motions. Recall that polytropic fluid balls can collapse homologously and form a singularity in finite time. We want to investigate whether or not elastic balls can collapse in a similar fashion. We will be using the polytropic elastic model from Section 4.5.

Using Definition 4 of an elastic ball in the Euler formulation, the system (2.20) becomes

$$\partial_t \delta + \frac{1}{r^2}\partial_r(r^2 \delta u) = 0, \tag{5.1a}$$

$$\mathcal{K}\delta(\partial_t u + u\partial_r u) = -a(\delta,\eta)\partial_r \delta + b(\delta,\eta)\frac{\eta-\delta}{r} - \frac{4\pi G}{3}\mathcal{K}^2 r\,\eta\,\delta, \tag{5.1b}$$

where

$$\eta(t,r) = \frac{3}{r^3}\int_0^r \delta(t,s)s^2\,ds \tag{5.1c}$$

and

$$a(\delta,\eta) = \partial_\delta \widehat{p}_{\mathrm{rad}}(\delta,\eta), \quad b(\delta,\eta) = 2\frac{\widehat{p}_{\tan}(\delta,\eta) - \widehat{p}_{\mathrm{rad}}(\delta,\eta)}{\eta-\delta} + 3\partial_\eta \widehat{p}_{\mathrm{rad}}(\delta,\eta). \tag{5.1d}$$

We again look for solutions of the form

$$\delta(t,r) = \frac{1}{\phi(t)^3}\delta_0\left(\frac{r}{\phi(t)}\right), \quad u(t,r) = \frac{\dot\phi(t)}{\phi(t)}r, \quad \phi(t)\neq 0.$$

Definition (5.1c) of $\eta$ then gives

$$\eta(t,r) = \frac{1}{\phi(t)^3}\eta_0\left(\frac{r}{\phi(t)}\right), \quad \eta_0(r) = \frac{3}{r^3}\int_0^r \delta_0(s)s^2\,ds,$$

and (5.1b) becomes

$$\begin{aligned}\mathcal{K}z\delta_0(z)\phi(t)\ddot\phi(t) = &-a(\phi(t)^{-3}\delta_0(z),\phi(t)^{-3}\eta_0(z))\delta_0'(z)\\ &+ b(\phi(t)^{-3}\delta_0(z),\phi(t)^{-3}\eta_0(z))\frac{\eta_0(z)-\delta_0(z)}{z}\\ &- \frac{4\pi G}{3}\mathcal{K}^2 z\delta_0(z)\eta_0(z)\phi(t)^{-1},\end{aligned} \tag{5.2}$$

Assuming that the elastic constitutive equation satisfies the scale invariance property (4.7), which is in particular satisfied by the polytropic elastic model, we obtain

$$\mathcal{K}\delta_0(z)z\phi(t)\ddot{\phi}(t) = \phi(t)^{-3\gamma}\left(-a(\delta_0(z),\eta_0(z))\delta_0'(z) + b(\delta_0(z),\eta_0(z))\frac{\eta_0(z)-\delta_0(z)}{z}\right) - \frac{4\pi G}{3}\mathcal{K}^2 z\delta_0(z)\eta_0(z)\phi(t)^{-1},$$

which can have solutions only if $\gamma = 1/3$ in which case the equation separates into the following system:

$$\phi(t)^2\ddot{\phi}(t) = \frac{4\pi\mathcal{K}G}{3}\alpha, \tag{5.3a}$$

$$a(\delta_0(z),\eta_0(z))\delta_0'(z) = b(\delta_0(z),\eta_0(z))\frac{\eta_0(z)-\delta_0(z)}{z} - \frac{4\pi G}{3}\mathcal{K}^2 z\delta_0(z)(\eta_0(z)+\alpha), \tag{5.3b}$$

$$\eta_0' = -\frac{3}{z}(\eta_0 - \delta_0), \tag{5.3c}$$

for some $\alpha \in \mathbb{R}$. The system (5.3) is supplied with initial data for $\phi$:

$$\phi(0) = \phi_0 = 1, \quad \dot{\phi}(0) = \phi_1$$

and with data at the center for $(\delta_0, \eta_0)$:

$$\delta_0(0) = \eta_0(0) = \delta_0^c > 0.$$

Equation (5.3a) is the same as in the fluid case and thus the properties of $\phi(t)$ are again described in Theorem 2 but with the critical value for $\phi_1$ replaced by

$$\phi_1^* = \sqrt{\frac{8\pi G\mathcal{K}|\alpha|}{3}}.$$

In elastic balls the pressure and density do not vanish at the same radius. This means we cannot write the radius as $R(t) = Z\phi(t)$, where $Z$ is the (finite) initial radius of the ball. Thus, boundary condition (2.23) that is necessary for conservation of total mass will no longer automatically be satisfied like it was in the fluid case.

We investigated the properties of solutions to (5.3) and found that in general they did not conserve the total mass of the ball. We constructed a collapsing ball with increasing mass, see Figure 5.1, and an eventually collapsing ball with decreasing mass, see Figure 5.2. In fact, based on these numerical results is has since been proved that the total mass is conserved if and only if the ball is static [4].

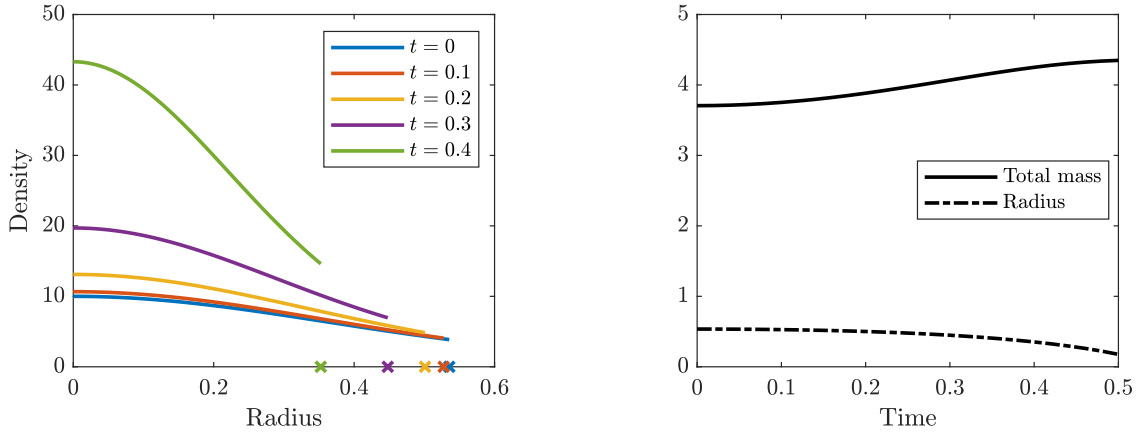


**Figure 5.1:** The pictures show the time evolution of a polytropic elastic ball with $\alpha = -1$, $\beta = 1$, $\nu = 0.1$, $\phi_1 = 0$, and $\rho_0^c = 10$. For clarity, crosses have been marked on the x-axis in the left picture to indicate where each curve ends, that is, they indicate the radius of the ball at each time step. The ball collapses while the mass increases. The y-axis in the right picture is not labeled because we have plotted both the total mass and the radius despite the different units.

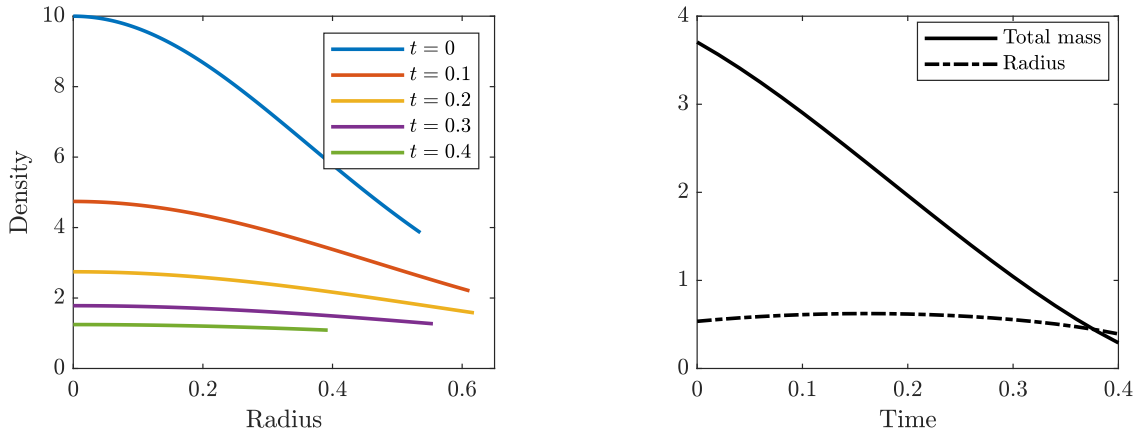


**Figure 5.2:** The pictures show the time evolution of a polytropic elastic ball with $\alpha = -1$, $\beta = 1$, $\nu = 0.1$, $\phi_1 = 3$, and $\rho_0^c = 10$. The ball initially expands then collapses while the mass decreases. The y-axis in the right picture is not labeled because we have plotted both the total mass and the radius despite the different units.

# 6

# Summary and Discussion

We summarize our findings. It is important to remember that numerical results are not proofs, but evidence nonetheless.

Regarding our first objective to study the questions left open in [1, 2] we have found numerical evidence supporting the following claims.

- Finite radius elastic balls cannot exist in the Saint Venant-Kirchhoff or Hadamard models if the hyperbolicity condition is violated at the center. See Figures 4.1 and 4.8.
- In the Hadamard model the condition $\delta_c < \Delta_\sharp$ on the central density in Theorem 5 can be replaced by the weaker $\delta_c < \Delta_\flat$. See Figures 4.7 and 4.8.
- In the quasi-linear John and Signorini models finite radius balls with $\delta_c < 1$ exist for certain values of the Poisson ratio $\nu$ when $\delta_c \in [\Delta_\circ(\nu), \Delta_*(\nu))$. See Figures 4.4 and 4.12.
- Finite radius balls always exist in the quasi-linear Signorini models when $\nu \in (-1, 0.5)$ and $\delta_c > 1$. See Figure 4.10.

In addition to addressing the open problems we made the following observation. The physically motivated Baker-Ericksen inequality remarkably does not seem to be satisfied everywhere in the Saint Venant-Kirchhoff and Hadamard models, see Figures 4.1 and 4.8. However, in our numerical solutions the inequality was only very slightly violated, and only when the central density was very close to violating the hyperbolicity condition, so this result could be due to numerical error and requires further investigation.

In the mass-radius diagrams we found that elastic balls typically do not have a one-to-one correspondence between mass and radius. This contrasts the polytropic fluid balls which, except for when $n = 1$ or $n = 3$, have a one-to-one correspondence between mass and radius.

Investigating the polytropic elastic model was our second objective and we were able to numerically construct balls of both type I, where solutions to the equations exist globally, and type II, where the solutions only exist locally, see Figure 4.14. The existence of global solutions is interesting because for polytropic fluids the solutions only exist locally on $[0, R]$.

We were also able to numerically construct shells and multi-body configurations in

the polytropic elastic model, see Figures 4.17 and 4.18.

Furthermore, we created mass-radius diagrams for balls constructed using different combinations of parameter values and found three main classes of diagrams.

- As the central density increases, the curve eventually turns around and starts approaching the origin, that is, both the mass and the radius eventually decrease.
- As the central density increases, the mass continues to increase while the radius instead decreases.
- As the central density increases, the curve eventually starts to spiral and seemingly converges a point in the diagram.

Based on our numerical evidence it seems that out of the five investigated models, the polytropic elastic model is the only one that sometimes admits mass-radius diagrams with spirals. Spirals are interesting because they also show up in mass-radius diagrams of self-gravitating elastic bodies in a relativistic setting, see [3].

Regarding our third objective to study the existence and properties of homologous elastic balls, we found that solutions existed in the polytropic elastic model (under the assumption that $\gamma = 1/3$) but that they did not conserve the total mass of the ball over time and thus violated one of the boundary conditions, see Figures 5.1 and 5.2.

However, we shall note the following. For polytropic fluid balls, the reference configuration is not a stress-free state since, if the reference density is given by $\rho = \mathcal{K} > 0$, then the pressure is given by $p = c\mathcal{K}^{1+1/n} > 0$ for some positive constants $c, n$. On the other hand, we imposed that the reference state of an elastic body should be stress-free, i.e., that $\widehat{p}_{\mathrm{rad}}(1,1) = \widehat{p}_{\tan}(1,1) = 0$. Based on our numerical discoveries the expression for the radial pressure has since been modified in the following way [4]:

$$\widehat{p}_{\mathrm{rad}}(\delta,\eta) = \delta^2 \partial_\delta w(\delta,\eta) + P,$$

where $P = \frac{\kappa}{1+\gamma}$ . It turns out that this slightly modified polytropic constitutive function results in a reference state that is no longer stress free but instead, the total mass of homologous elastic solutions is conserved.

This thesis is set entirely in Newtonian gravity. A possible direction to continue in next would be to expand the numerical investigations to elastic balls in a relativistic setting.

# Bibliography


[1] A. Alho and S. Calogero. Multi-body spherically symmetric steady states of Newtonian self-gravitating elastic matter. *Communications in Mathematical Physics*, 371(3):975–1004, 2019.

[2] A. Alho and S. Calogero. Static self-gravitating Newtonian elastic balls. *Archive for Rational Mechanics and Analysis*, 238(2):639–669, 2020.

[3] H. Andréasson and S. Calogero. Spherically symmetric steady states of John elastic bodies in general relativity. *Classical and Quantum Gravity*, 31(16):165008, 2014.

[4] S. Calogero. Dynamics of self-gravitating elastic balls. *In preparation*, 2020.

[5] N. Chamel and P. Haensel. Physics of neutron star crusts. *Living Reviews in relativity*, 11(1):10, 2008.

[6] S. Chandrasekhar. *An introduction to the study of stellar structure*, volume 2. Courier Corporation, 1957.

[7] C.-C. Fu and S.-S. Lin. On the critical mass of the collapse of a gaseous star in spherically symmetric and isentropic motion. *Japan journal of industrial and applied mathematics*, 15(3):461–469, 1998.

[8] H. Gercek. Poisson's ratio values for rocks. *International Journal of Rock Mechanics and Mining Sciences*, 44(1):1–13, 2007.

[9] P. Goldreich and S. V. Weber. Homologously collapsing stellar cores. *Astrophysical Journal*, 238(1):991–997, 1980.

[10] R. Kippenhahn, A. Weigert, and A. Weiss. *Stellar structure and evolution*, volume 192. Springer, 1990.

[11] L. Lichtenstein. *Gleichgewichtsfiguren rotierender flüssigkeiten*. Springer, 1933.

[12] T. Makino. On the existence of positive solutions at infinity for ordinary differential equations of Emden type. *Funkcialaj Ekvacioj*, 27(3):319–329, 1984.

[13] J. E. Marsden and T. J. Hughes. *Mathematical foundations of elasticity*. Courier Corporation, 1994.

[14] W. H. Müller and W. Weiss. *The State of Deformation in Earthlike Self-Gravitating Objects*. Springer, 2016.

[15] R. W. Ogden. *Non-linear elastic deformations*. Courier Corporation, 1997.

[16] T. Ramming and G. Rein. Spherically symmetric equilibria for self-gravitating kinetic or fluid models in the nonrelativistic and relativistic case—a simple proof for finite extension. *SIAM Journal on Mathematical Analysis*, 45(2):900–914, 2013.

[17] U. M. Schaudt. On static stars in Newtonian gravity and Lane-Emden type equations. In *Annales Henri Poincaré*, volume 1, pages 945–976. Springer, 2000.

# A

# Sample Code

Sample Matlab code for numerically constructing elastic balls in the Saint Venant-Kirchhoff material model.

```
% Constants and parameters
G       = 1;    % gravitational constant
K       = 1;    % reference density
kappa   = 1;    % bulk modulus
nu      = 1/4;  % Poisson ratio
rho_c   = 3;    % central density

% Setup domain of integration
r0      = 1e-50;
rmax    = 1;
rspan   = linspace(r0,rmax,1e5);

% Compute initial conditions at r0
deltaC  = rho_c/K;
y0      = approxIC(deltaC,kappa,nu,G,K,r0,@SVK);

% Set tolerances and option to terminate integration early
options = odeset('Events',@(r,y)pradZero(r,y,kappa,nu,@SVK),...
    'RelTol',1e-12,'AbsTol',1e-15);

% Solve for delta, eta, and m
[r,y]   = ode45(@(r,y)RHS(r,y,kappa,nu,G,K,@SVK),rspan,y0,options);
delta   = y(:,1);
eta     = y(:,2);
m       = y(:,3);

% Plot pressures, density, and local mass
[prad,ptan,~,~] = SVK(delta,eta,kappa,nu);
rho     = K*delta;
plot(r,prad,'k-',r,ptan,'k-.',r,rho,'k:',r,m,'k--','Linewidth',1.5);
legend('p_{rad}','p_{tan}','\rho','m');
xlabel('Radius');

```

```
% Functions

function [prad,ptan,ddeltaprad,detaprad] = SVK(delta,eta,kappa,nu)
% Saint Venant–Kirchhoff constitutive functions and partial
   derivatives
prad = 3*eta.^(2/3)*kappa.*(eta.^2*(nu-1)+delta.^2.*...
    (-2*nu+eta.^(2/3)*(1+nu))./(2*delta.^3*(1+nu));
ptan = 3*kappa*(-eta.^2*nu+delta.^2.*(-1+eta.^(2/3)*(1+nu))./...
    (2*delta.*eta.^(4/3)*(1+nu));
ddeltaprad = -3*eta.^(2/3)*kappa.*(3*eta.^2*(nu-1)+delta.^2.*...
    (-2*nu+eta.^(2/3)*(1+nu))./(2*delta.^4*(1+nu));
detaprad = 2*kappa*(2*eta.^2*(nu-1)+delta.^2.*...
    (-nu+eta.^(2/3)*(1+nu)))./(delta.^3.*eta.^(1/3)*(1+nu));
end

function dy = RHS(r,y,kappa,nu,G,K,ConFun)
% Right-hand side in system of ODEs
delta   = y(1);
eta     = y(2);
m       = y(3);
[prad,ptan,ddeltaprad,detaprad] = ConFun(delta,eta,kappa,nu);
ddelta  = (-3/r*detaprad*(delta-eta)-2/r*(prad-ptan)...
    -G*K*delta*m/r^2)/ddeltaprad;
deta    = 3/r*(delta-eta);
dm      = 4*pi*K*r^2*delta;
dy      = [ddelta;deta;dm];
end

function y0 = approxIC(deltaC,kappa,nu,G,K,r0,ConFun)
% Second order approximations of delta(r0), eta(r0), and m(r0)
[~,~,ddeltapradC,~] = ConFun(deltaC,deltaC,kappa,nu);
delta0  = deltaC - 2*pi*G*K^2/3 * deltaC.^2*r0^2./ddeltapradC;
eta0    = deltaC - 2*pi*G*K^2/5 * deltaC.^2*r0^2./ddeltapradC;
m0      = 0;
y0      = [delta0,eta0,m0];
end

function [value,isterminal,direction] = pradZero(~,y,kappa,nu,ConFun)
% Tells ode45 to terminate integration when prad reaches zero
delta       = y(1);
eta         = y(2);
prad        = ConFun(delta,eta,kappa,nu);
value       = prad;
isterminal  = 1;
direction   = 0;
end
```


CHALMERS
UNIVERSITY OF TECHNOLOGY